NOMA for Energy-Efficient LiFi-Enabled Bidirectional IoT Communication

Chen Chen, *Member, IEEE*, Shu Fu, Xin Jian, Min Liu, Xiong Deng, *Member, IEEE*, and Zhiguo Ding, *Fellow, IEEE*

***Abstract*— In this paper, we consider a light fidelity (LiFi)-enabled bidirectional Internet of Things (IoT) communication system, where visible light and infrared light are used in the downlink and uplink, respectively. In order to efficiently improve the energy efficiency (EE) of the bidirectional LiFi-IoT system, non-orthogonal multiple access (NOMA) with a quality-of-service (QoS)-guaranteed optimal power allocation (OPA) strategy is applied to maximize the EE of both downlink and uplink channels. We derive closed-form OPA sets based on the identification of the optimal decoding orders in both downlink and uplink channels, which can enable low-complexity power allocation. Moreover, we propose an adaptive channel and QoS-based user pairing approach by jointly considering users' channel gains and QoS requirements. We further analyze the EE and the user outage probability (UOP) performance of both downlink and uplink channels in the bidirectional LiFi-IoT system. Extensive analytical and simulation results demonstrate the superiority of NOMA with OPA in comparison to orthogonal multiple access (OMA) and NOMA with typical channel-based power allocation strategies. It is also shown that the proposed adaptive channel and QoS-based user pairing approach greatly outperforms individual channel/QoS-based approaches, especially when users have diverse QoS requirements.**

***Index Terms*— Non-orthogonal multiple access (NOMA), light fidelity (LiFi), Internet of Things (IoT), energy efficiency (EE), user outage probability (UOP).**

I. Introduction

With the explosive increase of smart devices in our everyday life, the Internet of Things (IoT) has been emerging as a promising solution to connect a large number of devices [1]. The IoT paradigm contains a variety of devices such as electronic devices, mobile devices and industrial devices, and different devices can have different communication and computation capabilities and quality-of-service (QoS) requirements [2]. As a key enabling technology of IoT, communication plays a vital role to connect all the smart devices supported in the IoT networks. Many radio frequency (RF)-based techniques have been considered for IoT communication such as RFID, ZigBee, Bluetooth, WiFi and 5G [3]. Recently, Light Fidelity (LiFi) has been envisioned as a promising IoT communication technology, which provides many attractive features that the RF-based IoT networks might struggle to offer, including accurate device positioning, energy harvesting from light and inherent physical-layer security [4]. As a lightwave-based communication technology, LiFi aims to realize a fully networked bidirectional wireless communication system by exploiting visible light in the downlink and infrared light in the uplink [5]. In particular, visible light-based LiFi downlink can be built upon the existing light emitting diode (LED) fixture which is widely deployed for general indoor lighting [6], [7].

A. Related Work and Motivation

Although LiFi reveals its potential for future IoT networks, the research of LiFi-enabled IoT is still at the early stage. In [8], a LiFi-based hierarchical IoT architecture was proposed to analyze the collected data and build smart decisions. In [9] and [10], the energy harvesting issues of LiFi-IoT were investigated. Lately, a LiFi-IoT system vision was reported in [4], where the conceptual architecture with four different types of motes was presented.

Considering that pervasive IoT is usually required to connect a huge number of IoT devices per unit area [4], the LiFi access point (AP) of an optical attocell in LiFi-IoT networks should be able to support multiple IoT devices. Therefore, an efficient multiple access technique is of great significance to successfully implement LiFi-IoT in practical scenarios. So far, many multiple access techniques have been introduced for visible light-based downlink LiFi communication, i.e., visible light communication (VLC), which can be mainly divided into two categories: one is orthogonal multiple access (OMA) and the other is non-orthogonal multiple access (NOMA). For OMA schemes such as frequency division multiple access/orthogonal frequency division multiple access (FDMA/OFDMA) and time division multiple access (TDMA), users are allocated with different orthogonal frequency or time resources [11]–[13]. Although OMA can eliminate mutual interference between users, its resource utilization is inefficient. In contrast, NOMA

Manuscript received May 24, 2020; revised November 22, 2020; accepted January 8, 2021. Date of publication January 18, 2021; date of current version March 17, 2021. This work was supported in part by the National Natural Science Foundation of China under Grant 61901065 and Grant 61701054, and in part by the Fundamental Research Funds for the Central Universities under Grant 2020CDJQY-A001 and Grant 2020CDJGFWDZ014. The associate editor coordinating the review of this article and approving it for publication was M. Safari. *(Corresponding author: Chen Chen.)*

Chen Chen and Shu Fu are with the School of Microelectronics and Communication Engineering, Chongqing University, Chongqing 400044, China, and also with the State Key Laboratory of Integrated Services Networks, Xidian University, Xi'an 710071, China (e-mail: c.chen@cqu.edu.cn; shufu@cqu.edu.cn).

Xin Jian and Min Liu are with the School of Microelectronics and Communication Engineering, Chongqing University, Chongqing 400044, China (e-mail: jianxin@cqu.edu.cn; liumin@cqu.edu.cn).

Xiong Deng is with the Department of Electrical Engineering, Eindhoven University of Technology (TU/e), 5600MB Eindhoven, The Netherlands (e-mail: x.deng@tue.nl).

Zhiguo Ding is with the School of Electrical and Electronic Engineering, The University of Manchester, Manchester M13 9PL, U.K. (e-mail: zhiguo.ding@manchester.ac.uk).

Color versions of one or more figures in this article are available at https://doi.org/10.1109/TCOMM.2021.3051912.

Digital Object Identifier 10.1109/TCOMM.2021.3051912

allows multiple users to simultaneously utilize all the frequency and time resources through power domain superposition coding (SPC) and successive interference cancellation (SIC) [14]. Due to its efficient resource utilization, NOMA has been recognized as a promising multiple access technique for multi-user VLC systems [15]–[20].

It has been shown that the performance gain of NOMA over OMA is mainly determined by both the power allocation strategy and the user pairing approach adopted in NOMA [21]. For NOMA-based multi-user VLC systems, various channel-based power allocation strategies have been proposed such as gain ratio power allocation (GRPA) and normalized gain difference power allocation (NGDPA) [14], [18]. Moreover, channel-based user pairing approaches have also been proposed to efficiently divide users into pairs [22], [23]. Nevertheless, all the aforementioned works only focused on the application of NOMA in visible light-based LiFi downlink channels. To apply NOMA in LiFi-enabled bidirectional IoT communication, the following two important issues should be taken into consideration:

1) Energy Consumption: In LiFi-enabled bidirectional IoT communication, energy consumption originates from two parts: one is the LiFi AP within each optical attocell and the other is the connected IoT devices. Particularly, most IoT devices rely on batteries and reducing the energy consumption to extend their battery life is a top concern [2], [3]. Therefore, it is of practical significance to design an energy-efficient multiple access technique for bidirectional LiFi-IoT.

2) Diverse Device QoS Requirements: In practical LiFi-IoT systems, the connected IoT devices can be generally divided into two categories: one includes low-speed devices such as environmental sensors and health monitors, and the other consists of high-speed devices such as multimedia-capable mobile phones [2], [24]. As a result, it is necessary to take the diverse QoS requirements of IoT devices into account when designing a multiple access technique for bidirectional LiFi-IoT.

B. Main Contributions

To address above-mentioned issues when applying NOMA, in this paper, we propose an energy-efficient NOMA technique for bidirectional LiFi-IoT communication. The main contributions of this work are summarized as follows:

- An energy-efficient NOMA technique is applied for the bidirectional LiFi-IoT system, which adopts a QoS-guaranteed optimal power allocation (OPA) strategy to maximize the energy efficiency (EE) of both downlink and uplink channels. The optimal decoding orders in the downlink and uplink channels are first identified and proved, and then the corresponding OPA sets are obtained in a simple and closed form, which can enable low-complexity power allocation.
- Three user pairing approaches are studied in the NOMA-enabled bidirectional LiFi-IoT system, including channel-based, QoS-based, and adaptive channel and QoS-based approaches. The newly proposed adaptive channel and QoS-based user pairing approach can dynamically select from the channel-based and the QoS-based approaches to achieve a higher EE.
- Both EE and user outage probability (UOP) are analyzed in the bidirectional LiFi-IoT system using different multiple access techniques. It is analytically proved that NOMA with OPA always achieves higher EE than OMA and NOMA with typical channel-based power allocation strategies (such as GRPA and NGDPA [14], [18]) in both downlink and uplink channels. The calculations of downlink and uplink UOPs are also discussed.
- Extensive analytical and simulation results are presented to evaluate the performance of different multiple access techniques in a typical bidirectional LiFi-IoT system. The obtained results demonstrate the superiority of NOMA adopting OPA with adaptive channel and QoS-based user pairing for energy-efficient bidirectional LiFi-IoT systems.

The remainder of this paper is organized as follows. Section II presents the system model. The principle of NOMA and its application for energy-efficient bidirectional LiFi-IoT communication are described in Section III. The EE and UOP of the bidirectional LiFi-IoT system using different multiple access techniques are analyzed in Section IV. Detailed analytical and simulation results are presented in Section V. Finally, Section VI concludes the paper.

II. System Model

We present the basic model of the bidirectional LiFi-IoT system in this section. The configuration of the bidirectional LiFi-IoT system is first introduced, and then the light propagation model and the noise model are further discussed.

A. Bidirectional LiFi-IoT System Configuration

In this work, we consider a single-cell bidirectional LiFi-IoT system,[1] where visible light is used in the downlink for simultaneous illumination and communication, while infrared light is adopted for uplink communication. Fig. 1 illustrates the geometric configuration of the bidirectional LiFi-IoT system with one LiFi AP and totally K users, i.e., IoT devices. As we can see, the LiFi AP consists of a visible light LED transmitter and an infrared light photodiode (PD) receiver, while each user is equipped with a visible light PD receiver and an infrared light LED transmitter. In the downlink, the visible light LED of the LiFi AP radiates white light to provide lighting within its coverage and broadcast downlink data to all the users at the same time. Each user detects the broadcasted data by using the equipped visible light PD. In the uplink, each user employs the equipped infrared light LED to transmit its uplink data and the LiFi AP utilizes the infrared light PD to collect the data from all the users. Therefore, the bidirectional communication between the LiFi AP and all the users in the LiFi-IoT system can be established.

Without loss of generality, we assume that both the visible and infrared light LEDs are point sources and they operate within their linear dynamic range. We further assume that

[1]Although a simple single-cell scenario is considered here, the obtained results are applicable to general multi-cell scenarios since inter-cell interference can be efficiently mitigated by applying spectrum partitioning, i.e., allocating adjacent LiFi APs with different subbands/subcarriers in the frequency domain [25], [26].

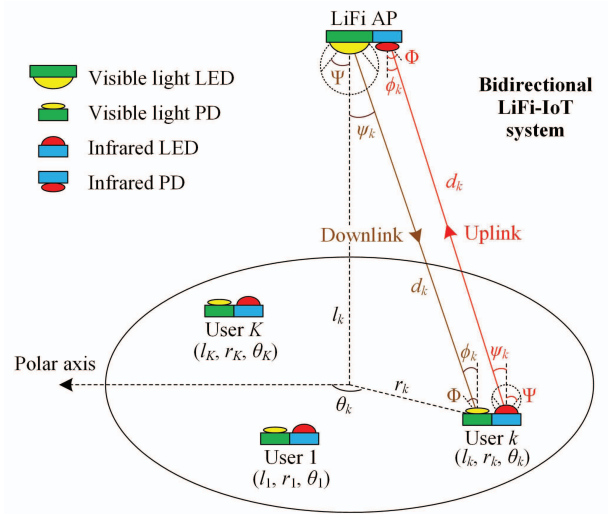

Fig. 1. Geometric configuration of the bidirectional LiFi-IoT system with one LiFi AP and K users, i.e., IoT devices.

the overall system has a flat frequency response.[2] Moreover, we also assume that the visible light LED and the infrared light PD of the LiFi AP are oriented vertically downwards, while the visible light PD and the infrared light LED of each user are oriented vertically upwards. For simplicity, we assume that the visible/infrared light LEDs have the same conversion efficiency and semi-angle, while the visible/infrared light PDs have the same responsivity and active area. Under the above assumptions, the models for visible light downlink and infrared light uplink channels become exactly the same [30].

B. Light Propagation Model

In practical LiFi-IoT systems, the visible light PD in the downlink and the infrared light PD in the uplink can receive both line-of-sight (LOS) and non-LOS components of the corresponding transmitted optical signals. Nevertheless, since the non-LOS component usually has much lower electrical power than that of the LOS component, it is generally reasonable to neglect the non-LOS component during most channel conditions [31]. For simplicity, we only consider the LOS component in the following channel model.

For the visible and infrared light LEDs with a Lambertian emission pattern, the LOS direct current (DC) channel gain between the LiFi AP and the k-th ($k = 1, 2, \cdots, K$) user for both downlink and uplink channels can be calculated by [6], [32], [33]

$$h_k = \begin{cases} \dfrac{(m+1)\beta\rho A}{2\pi d_k^2}\cos^m(\psi_k) g_f g_c \cos(\phi_k), & 0 \le \phi_k \le \Phi \\ 0, & \phi_k > \Phi \end{cases}, \tag{1}$$

where $m = -\ln 2/\ln(\cos(\Psi))$ denotes the Lambertian emission order with Ψ being the semi-angle of the visible/infrared light LED; β and ρ represent the current-to-light conversion efficiency of the visible/infrared light LED and the responsivity of the visible/infrared light PD, respectively; A is the active area of the visible/infrared light PD; d_k is the distance between the LiFi AP and the k-th user; ψ_k and ϕ_k denote the corresponding emission angle and incident angle, respectively; g_f and g_c represent the gains of the optical filter and the optical concentrator, respectively. The gain of the optical concentrator can be calculated by $g_c = \frac{n^2}{\sin^2\Phi}$, where n is the refractive index of the optical concentrator and Φ is the half-angle field-of-view (FOV) of the receiver.

Considering the fact that different users might have different heights in practical LiFi-IoT systems, the locations of users should be within a three-dimensional (3D) space. For a better description of the 3D location of a user, the polar coordinate system is adopted as shown in Fig. 1. In the polar coordinate system, the 3D location of the k-th user can be represented by (l_k, r_k, θ_k), where l_k and r_k respectively denote its vertical and horizontal distances from the LiFi AP, and θ_k denotes its polar angle from the reference axis.

As shown in Fig. 1, due to the assumption that the LiFi AP is oriented vertically downwards while each user is oriented vertically upwards, the emission angle and the incident angle corresponding to the LiFi AP and the k-th user become the same, i.e., $\psi_k = \phi_k$. Hence, ψ_k and ϕ_k can be represented by $\psi_k = \phi_k = \arctan\left(\frac{r_k}{l_k}\right)$. Moreover, d_k can be expressed by $d_k = \sqrt{l_k^2 + r_k^2}$. Therefore, h_k can be rewritten as follows:

$$h_k = \begin{cases} \dfrac{\mathcal{C}}{l_k^2 + r_k^2}\cos^{m+1}\left(\arctan\left(\frac{r_k}{l_k}\right)\right), & 0 \le \frac{r_k}{l_k} \le \tan\Phi \\ 0, & \frac{r_k}{l_k} > \tan\Phi \end{cases}, \tag{2}$$

where $\mathcal{C} = \frac{(m+1)\beta\rho A g_f g_c}{2\pi}$. It can be found from (2) that h_k is dependent on both the vertical distance l_k and the horizontal distance r_k, which is not affected by the polar angle θ_k.

C. Noise Model

The additive noises in both downlink and uplink channels consist of thermal and shot noises, which are generally modeled as real-valued zero-mean additive white Gaussian noises. For simplicity, it is assumed that the additive noises in both downlink and uplink channels have the same constant noise power spectral density (PSD) N_0. For an overall system bandwidth B_s, the noise powers in both downlink and uplink channels can be obtained as $P_z = N_0\ B_s$.

III. NOMA FOR BIDIRECTIONAL LiFi-IoT

A. Principle of NOMA

Fig. 2 illustrates the conceptual diagrams of FDMA/OFDMA, TDMA and NOMA with two users, and the QoS requirements for user 1 and user 2 are represented by "QoS 1" and "QoS 2", respectively. For the case of FDMA/OFDMA, the subbands/subcarriers are orthogonal to each other, and therefore the QoS requirement of a specific user can be ensured by allocating it with a proper number of subbands/subcarriers, i.e., a proper bandwidth. As shown in Fig. 2(a), user 1 and user 2 are allocated with bandwidths B_1 and B_2 to satisfy their QoS requirements, respectively. Due to the orthogonality of all the subbands/subcarriers, there is no mutual interference between the transmitted data of two users. Nevertheless, interference-free multiple access is

[2]Note that this assumption can be easily ensured by applying efficient frequency-domain equalization techniques [27]–[29].

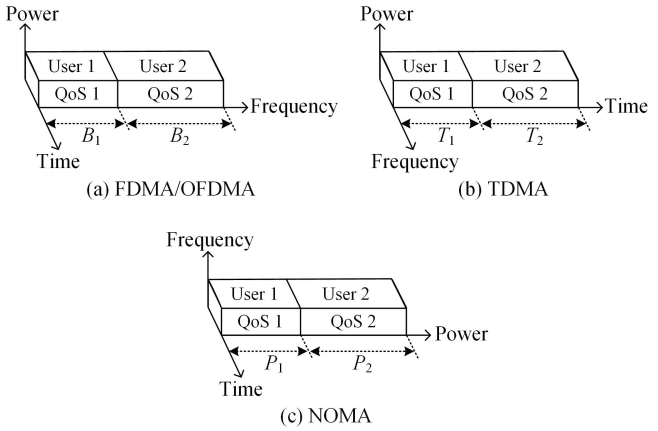

Fig. 2. Conceptual diagram of (a) FDMA/OFDMA, (b) TDMA and (c) NOMA.

achieved by splitting the overall bandwidth into two parts. For the case of TDMA, as shown in Fig. 2(b), time slots T_1 and T_2 are allocated for user 1 and user 2 to meet their QoS requirements, respectively. Since time slots T_1 and T_2 are independent of each other, the transmitted data of two users are not mutually interfered. Hence, the mutual interference is eliminated by splitting the overall time resource into two parts. It can be concluded that the frequency or time resources must be split and shared so as to support multiple users without mutual interference for OMA schemes such as FDMA/OFDMA and TDMA.

In contrast to OMA, NOMA allows both users to utilize all the frequency and time resources. It can be viewed from Fig. 2(c) that the transmitted data of user 1 and user 2 are superposed in the power domain and there inevitably exists mutual interference. To ensure their QoS requirements, user 1 and user 2 are allocated with powers P_1 and P_2, respectively. It has been well shown that the performance of NOMA is largely dependent on the adopted power allocation strategy [21]. In conventional NOMA-based systems, the power allocation strategy is designed to maximize the sum rate of the system under a total transmit power constraint. However, when applying NOMA for energy-sensitive IoT applications, the power allocation strategy should be designed from the energy consumption perspective.

When there are more than two users in the system, they are generally divided into multiple pairs and a hybrid NOMA/OMA scheme can be adopted to support multiple user pairs [22], [23]. Specifically, the two users within each user pair are multiplexed in the power domain via NOMA while different user pairs are multiplexed in the frequency/time domain via OMA. When applying FDMA/OFDMA to multiplex different user pairs, each user pair is allocated with an independent portion of the overall system bandwidth (i.e., orthogonal subbands/subcarriers). Hence, there is no interference between different user pairs owing to the orthogonality in the frequency domain. Moreover, due to the assumption that the overall system has a flat frequency response, the power requirements of each user pair are not affected by the low-pass frequency response of the LED transmitters, which can be individually and independently obtained according to its specific QoS requirements and channel conditions. Therefore, the power requirements of all the users in both downlink and uplink channels of the NOMA-enabled bidirectional LiFi-IoT system are derived pairwisely in the following two subsections.

B. NOMA for Downlink LiFi-IoT Using Visible Light

In this subsection, NOMA is introduced for downlink LiFi-IoT communication using visible light. Without loss of generality, we assume that the bidirectional LiFi-IoT system serves $K = 2$ N users,[3] which are divided into N user pairs. Fig. 3(a) shows the schematic diagram of NOMA-enabled LiFi-IoT downlink. Let $s^{\mathrm{d}}_{i,f}$ and $s^{\mathrm{d}}_{i,n}$ denote the modulated message signals intended for the far and near users in the i-th user pair, respectively. Here, the superscript "d" denotes the LiFi-IoT downlink, while the subscripts "f" and "n" stand for the far and near users, respectively. For the two users within each user pair, intra-pair power domain superposition is performed. Hence, the superposed electrical signal of the i-th user pair can be expressed by

$$x^{\mathrm{d}}_i = \sqrt{p^{\mathrm{d}}_{i,f}} s^{\mathrm{d}}_{i,f} + \sqrt{p^{\mathrm{d}}_{i,n}} s^{\mathrm{d}}_{i,n}, \tag{3}$$

where $p^{\mathrm{d}}_{i,f}$ and $p^{\mathrm{d}}_{i,n}$ are the downlink electrical transmit powers allocated to the far and near users in the i-th user pair, respectively. Hence, the total downlink electrical transmit power allocated to all N pairs of users is obtained by $P^{\mathrm{d}}_{\mathrm{elec}} = \sum_{i=1}^{N} p^{\mathrm{d}}_{i,f} + p^{\mathrm{d}}_{i,n}$. After intra-pair power domain superposition, OFDMA-based inter-pair bandwidth allocation is further performed in the frequency domain, where the i-th user pair is assumed to be allocated with a bandwidth B^{d}_i and thus the required overall system bandwidth is given by $B^{\mathrm{d}}_{\mathrm{elec}} = \sum_{i=1}^{N} B^{\mathrm{d}}_i$. Subsequently, a DC bias current $I^{\mathrm{d}}_{\mathrm{DC}}$ is added to the resultant signal so as to simultaneously ensure the non-negativity of the driving signal of the visible light LED and guarantee sufficient and stable illumination.

After removing the DC term, the received downlink signals of the far and near users in the i-th user pair can be given by

$$\begin{cases} y^{\mathrm{d}}_{i,f} = h^{\mathrm{d}}_{i,f}(\sqrt{p^{\mathrm{d}}_{i,f}} s^{\mathrm{d}}_{i,f} + \sqrt{p^{\mathrm{d}}_{i,n}} s^{\mathrm{d}}_{i,n}) + z^{\mathrm{d}}_{i,f} \\ y^{\mathrm{d}}_{i,n} = h^{\mathrm{d}}_{i,n}(\sqrt{p^{\mathrm{d}}_{i,f}} s^{\mathrm{d}}_{i,f} + \sqrt{p^{\mathrm{d}}_{i,n}} s^{\mathrm{d}}_{i,n}) + z^{\mathrm{d}}_{i,n} \end{cases}, \tag{4}$$

where $h^{\mathrm{d}}_{i,f}$ and $h^{\mathrm{d}}_{i,n}$ denote the downlink channel gains of the far and near users in the i-th user pair, respectively, and $h^{\mathrm{d}}_{i,f} \leq h^{\mathrm{d}}_{i,n}$; $z^{\mathrm{d}}_{i,f}$ and $z^{\mathrm{d}}_{i,n}$ are the corresponding additive noises.

To decode the intended message signals for the far and near users in the i-th user pair, the decoding order should be first obtained. Here, we assume that the two users are sorted as a high priority user and a low priority user based on a specific sorting criteria, i.e., the decoding order can be generally given by $\mathbb{O}^{\mathrm{d}}_{i,\mathrm{high}} \geq \mathbb{O}^{\mathrm{d}}_{i,\mathrm{low}}$. The determination of the optimal decoding order will be discussed in Section III.D. Moreover, different users might have different QoS requirements in practical LiFi-IoT systems. Generally, we can define the QoS requirement of a specific user as its required achievable rate per bandwidth, i.e., spectral efficiency [15]. Let $\widetilde{R}^{\mathrm{d}}_{i,\mathrm{high}}$ and

[3] Although an even number of users is considered here, NOMA is generally applicable to an arbitrary number of users. For an odd number of users, they are first sorted and then divided into pairs, and the remaining unpaired user can be allocated with separate power and bandwidth resources [23].

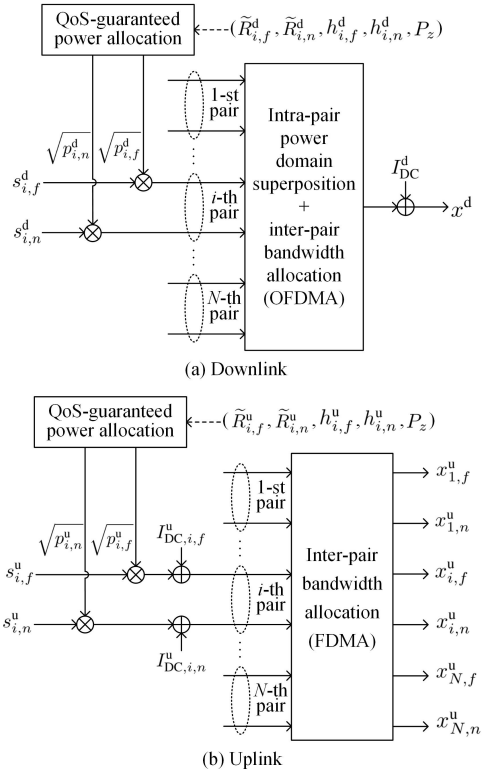

Fig. 3. Schematic diagram of NOMA-enabled LiFi-IoT (a) downlink and (b) uplink.

$\widetilde{R}^{\mathrm{d}}_{i,\mathrm{low}}$ denote the rate requirements of the high and low priority users in the i-th user pair in the downlink, respectively. The corresponding power requirements for both users in the i-th user pair in the downlink to meet their QoS requirements are given by the following theorem.

Theorem 1: For the high and low priority users in the i-th user pair with arbitrary QoS requirements in the downlink of the bidirectional LiFi-IoT system, the power requirements to satisfy their QoS requirements are given by

$$\begin{cases} p^{\mathrm{d}}_{i,\mathrm{high}} \geq \mathbb{R}^{\mathrm{d}}_{i,\mathrm{high}} \left(\mathbb{R}^{\mathrm{d}}_{i,\mathrm{low}} \frac{P_z}{(h^{\mathrm{d}}_{i,\mathrm{low}})^2} + \frac{P_z}{(h^{\mathrm{d}}_{i,\mathrm{min}})^2} \right) \\ p^{\mathrm{d}}_{i,\mathrm{low}} \geq \mathbb{R}^{\mathrm{d}}_{i,\mathrm{low}} \frac{P_z}{(h^{\mathrm{d}}_{i,\mathrm{low}})^2} \end{cases}, \tag{5}$$

where $\mathbb{R}^{\mathrm{d}}_{i,\mathrm{high}} = 2^{2\widetilde{R}^{\mathrm{d}}_{i,\mathrm{high}}} - 1$, $\mathbb{R}^{\mathrm{d}}_{i,\mathrm{low}} = 2^{2\widetilde{R}^{\mathrm{d}}_{i,\mathrm{low}}} - 1$, $h^{\mathrm{d}}_{i,\mathrm{min}} = \min\{h^{\mathrm{d}}_{i,\mathrm{high}}, h^{\mathrm{d}}_{i,\mathrm{low}}\}$ and P_z is the noise power defined in Section II.C.

Proof: Please refer to the appendix. ∎

Theorem 1 demonstrates that the QoS requirements of the high and low priority users in the i-th user pair in the downlink can be guaranteed under the impact of mutual interference by allocating them with proper powers.

C. NOMA for Uplink LiFi-IoT Using Infrared Light

Besides the downlink LiFi-IoT communication as discussed above, NOMA can also be applied for uplink LiFi-IoT communication using infrared light.[4] The schematic diagram of NOMA-enabled LiFi-IoT uplink is plotted in Fig. 3(b). Let $s^{\mathrm{u}}_{i,f}$ and $s^{\mathrm{u}}_{i,n}$ be the modulated uplink message signals intended for the LiFi AP from the far and near users in the i-th user pair, respectively, with the superscript "u" denoting the LiFi-IoT uplink. The electrical signals to be transmitted by the infrared light LEDs of the far and near users in the i-th user pair can be expressed by

$$\begin{cases} x^{\mathrm{u}}_{i,f} = \sqrt{p^{\mathrm{u}}_{i,f}} s^{\mathrm{u}}_{i,f} + I^{\mathrm{u}}_{\mathrm{DC},i,f} \\ x^{\mathrm{u}}_{i,n} = \sqrt{p^{\mathrm{u}}_{i,n}} s^{\mathrm{u}}_{i,n} + I^{\mathrm{u}}_{\mathrm{DC},i,n} \end{cases}, \tag{6}$$

where $p^{\mathrm{u}}_{i,f}$ and $p^{\mathrm{u}}_{i,n}$ are the uplink electrical transmit powers of the far and near users in the i-th user pair, respectively; $I^{\mathrm{u}}_{\mathrm{DC},i,f}$ and $I^{\mathrm{u}}_{\mathrm{DC},i,n}$ are the DC bias currents added to guarantee the non-negativity of the driving signals of the infrared LEDs. The total uplink electrical transmit power of all N pairs of users is given by $P^{\mathrm{u}}_{\mathrm{elec}} = \sum_{i=1}^{N} p^{\mathrm{u}}_{i,f} + p^{\mathrm{u}}_{i,n}$. For the N pairs of users in the uplink, due to the asynchronous transmission nature of LiFi uplink channels, FDMA-based inter-pair bandwidth allocation is carried out in the frequency domain. Assuming the i-th user pair is allocated with a bandwidth B^{u}_i, the required overall system bandwidth can be obtained by $B^{\mathrm{u}}_{\mathrm{elec}} = \sum_{i=1}^{N} B^{\mathrm{u}}_i$.

At the LiFi AP, the received uplink signal of the i-th user pair after removing the DC term can be expressed by

$$y^{\mathrm{u}}_i = h^{\mathrm{u}}_{i,f} \sqrt{p^{\mathrm{u}}_{i,f}} s^{\mathrm{u}}_{i,f} + h^{\mathrm{u}}_{i,n} \sqrt{p^{\mathrm{u}}_{i,n}} s^{\mathrm{u}}_{i,n} + z^{\mathrm{u}}_i, \tag{7}$$

where $h^{\mathrm{u}}_{i,f}$ and $h^{\mathrm{u}}_{i,n}$ are the uplink channel gains of the far and near users in the i-th user pair, respectively, and $h^{\mathrm{u}}_{i,f} \leq h^{\mathrm{u}}_{i,n}$; z^{u}_i is the corresponding additive noise.

Similarly, we assume that the far and near users in the i-th user pair in the uplink are sorted as a high priority user and a low priority user with the decoding order $\mathbb{O}^{\mathrm{u}}_{i,\mathrm{high}} \geq \mathbb{O}^{\mathrm{u}}_{i,\mathrm{low}}$. In addition, the QoS requirements of the high and low priority users in the i-th user pair are given by $\widetilde{R}^{\mathrm{u}}_{i,\mathrm{high}}$ and $\widetilde{R}^{\mathrm{u}}_{i,\mathrm{low}}$, respectively. The following theorem gives the power requirements for the high and low priority users in the i-th user pair in the uplink to meet their QoS requirements.

Theorem 2: For the high and low priority users in the i-th user pair with arbitrary QoS requirements in the uplink of the bidirectional LiFi-IoT system, the required powers to meet their QoS requirements are given by

$$\begin{cases} p^{\mathrm{u}}_{i,\mathrm{high}} \geq \mathbb{R}^{\mathrm{u}}_{i,\mathrm{high}} (\mathbb{R}^{\mathrm{u}}_{i,\mathrm{low}} + 1) \frac{P_z}{(h^{\mathrm{u}}_{i,\mathrm{high}})^2} \\ p^{\mathrm{u}}_{i,\mathrm{low}} \geq \mathbb{R}^{\mathrm{u}}_{i,\mathrm{low}} \frac{P_z}{(h^{\mathrm{u}}_{i,\mathrm{low}})^2} \end{cases}, \tag{8}$$

where $\mathbb{R}^{\mathrm{u}}_{i,\mathrm{high}} = 2^{2\widetilde{R}^{\mathrm{u}}_{i,\mathrm{high}}} - 1$, $\mathbb{R}^{\mathrm{u}}_{i,\mathrm{low}} = 2^{2\widetilde{R}^{\mathrm{u}}_{i,\mathrm{low}}} - 1$ and P_z is the corresponding noise power.

Proof: Please refer to the appendix. ∎

It is demonstrated by Theorem 2 that, by adopting a proper power allocation strategy, the QoS requirements of the mutually interfered high and low priority users in the i-th user pair in the uplink can be successfully guaranteed.

D. QoS-Guaranteed Optimal Power Allocation (OPA)

For the efficient implementation of NOMA in bidirectional LiFi-IoT systems, a QoS-guaranteed OPA strategy is derived in this subsection. In practical LiFi-IoT systems, each user

[4]Although RF technologies can also be applied in the uplink to build a hybrid system [34]–[37], the use of infrared light in the uplink has attractive advantages such as no electromagnetic interference radiation and potentially high data rate [4]. Moreover, the eye safety issue can be addressed by carefully setting the emit power and the FOV of the infrared light, and the blockage issue can be tackled by adopting hybrid WiFi/LiFi transmission [5], [36].

has its own QoS requirements, i.e., rate requirements, in both downlink and uplink channels. As a result, a bidirectional LiFi-IoT system is considered working properly, as long as the QoS requirements of all the users are satisfied. This is quite different from conventional NOMA-based systems, since their common goal is to maximize the achievable sum rate of all the users under a total transmit power constraint [38]. As energy consumption is a very important factor that needs to be considered when designing an IoT system, it is of practical significance to reduce the energy consumption of the system without compromising its working performance. From the energy consumption perspective, the goal to design NOMA-enabled bidirectional LiFi-IoT systems is to maximize the EE in both downlink and uplink channels via a QoS-guaranteed OPA strategy. Generally, the EE (η^b) with unit bits/J/Hz in the downlink/uplink channel can be defined as the ratio of the achievable sum rate (R^b) to the total electrical power consumption (P^b_{elec}):

$$\eta^b = \frac{R^b}{P^b_{\text{elec}}}, \tag{9}$$

where $P^b_{\text{elec}} = \sum_{i=1}^{N} p^b_{i,f} + p^b_{i,n}$, and $b \in \{\text{d}, \text{u}\}$ with "d" and "u" denoting the downlink and uplink channels, respectively.

For the NOMA-enabled bidirectional LiFi-IoT system with N pairs of users, the target sum rate of the downlink/uplink channel can be calculated by $R^b = \sum_{i=1}^{N} \widetilde{R}^b_{i,f} + \widetilde{R}^b_{i,n}$ with $b \in \{\text{d}, \text{u}\}$, where $\widetilde{R}^b_{i,f}$ and $\widetilde{R}^b_{i,n}$ denote the rate requirements of the far and near users in the i-th user pair in the downlink/uplink channel, respectively.

1) Optimal Decoding Order: To obtain the desired OPA strategy, the optimal decoding orders for the far and near users in the i-th user pair in both downlink and uplink channels should be first identified. Based on the derived power requirements in (5) and (8), the optimal decoding orders are given by the following proposition.

Proposition 1: The optimal decoding orders for the far and near users in the i-th user pair in the downlink and uplink channels of the bidirectional LiFi-IoT system are given by $\mathbb{O}^{\text{d}}_{i,f} \geq \mathbb{O}^{\text{d}}_{i,n}$ and $\mathbb{O}^{\text{u}}_{i,f} < \mathbb{O}^{\text{u}}_{i,n}$, respectively.

Proof: Please refer to the appendix. ∎

According to Proposition 1, the power requirements for the far and near users in the i-th user pair in the downlink channel of the bidirectional LiFi-IoT system can be obtained by

$$\begin{cases} p^{\text{d}}_{i,f} \geq \mathbb{R}^{\text{d}}_{i,f} \left(\mathbb{R}^{\text{d}}_{i,n} \dfrac{P_z}{(h^{\text{d}}_{i,n})^2} + \dfrac{P_z}{(h^{\text{d}}_{i,f})^2} \right) \\ p^{\text{d}}_{i,n} \geq \mathbb{R}^{\text{d}}_{i,n} \dfrac{P_z}{(h^{\text{d}}_{i,n})^2} \end{cases}, \tag{10}$$

and the power requirements for the far and near users in the i-th user pair in the uplink channel is further given by

$$\begin{cases} p^{\text{u}}_{i,f} \geq \mathbb{R}^{\text{u}}_{i,f} \dfrac{P_z}{(h^{\text{u}}_{i,f})^2} \\ p^{\text{u}}_{i,n} \geq \mathbb{R}^{\text{u}}_{i,n} (\mathbb{R}^{\text{u}}_{i,f} + 1) \dfrac{P_z}{(h^{\text{u}}_{i,n})^2}. \end{cases} \tag{11}$$

2) Problem Formulation: Let $\mathcal{P}^b_i = \{p^b_{i,f}, p^b_{i,n}\}$ with $b \in \{\text{d}, \text{u}\}$ denote the power allocation sets for the far and near users in the i-th user pair in the downlink/uplink channel. To obtain the desired QoS-guaranteed OPA strategy (i.e., optimal $\mathcal{P}^{\text{d,OPA}}_i$ with $i = 1, 2, \cdots, N$) in the downlink channel, the EE maximization problem can be formulated as

$$\begin{aligned} \max_{\{\mathcal{P}^{\text{d,OPA}}_1, \cdots, \mathcal{P}^{\text{d,OPA}}_N\}} \ & \eta^{\text{d}} \\ \text{s.t.} \ \ & \text{C1: } (10) \\ & \text{C2: } P^{\text{d}}_{\text{elec}} \leq P^{\text{d}}_{\max}, \end{aligned} \tag{12}$$

where constraint "C1" is to guarantee the power requirements of all the downlink users so as to meet their QoS requirements and constraint "C2" is that the total downlink electrical transmit power of the LiFi AP should not exceed its maximum value $P^{\text{d}}_{\max}$. Similarly, to obtain optimal $\mathcal{P}^{\text{u,OPA}}_i$ with $i = 1, 2, \cdots, N$, the EE maximization problem in the uplink channel can be formulated as

$$\begin{aligned} \max_{\{\mathcal{P}^{\text{u,OPA}}_1, \cdots, \mathcal{P}^{\text{u,OPA}}_N\}} \ & \eta^{\text{u}} \\ \text{s.t.} \ \ & \text{C3: } (11) \\ & \text{C4: } p^{\text{u}}_{i,f} \leq p^{\text{u}}_{\max} \\ & \text{C5: } p^{\text{u}}_{i,n} \leq p^{\text{u}}_{\max}, \end{aligned} \tag{13}$$

where constraint "C3" is to ensure the power requirements of all the uplink users, and constraints "C4" and "C5" are imposed to ensure that the uplink electrical transmit power does not exceed the maximum value $p^{\text{u}}_{\max}$.

Considering the fact that each user in the bidirectional LiFi-IoT system normally has its fixed downlink/uplink QoS requirement during a certain period of time, the target sum rate R^b with $b \in \{\text{d}, \text{u}\}$ in the downlink/uplink channel can be viewed as a fixed value during this time period. Therefore, the EE maximization problems in (12) and (13) can be respectively transformed into two power minimization problems which are given as follows:

$$\begin{aligned} \min_{\{\mathcal{P}^{\text{d,OPA}}_1, \cdots, \mathcal{P}^{\text{d,OPA}}_N\}} \ & P^{\text{d}}_{\text{elec}} \\ \text{s.t.} \ \ & \text{C1: } (10) \\ & \text{C2: } P^{\text{d}}_{\text{elec}} \leq P^{\text{d}}_{\max}, \end{aligned} \tag{14}$$

$$\begin{aligned} \min_{\{\mathcal{P}^{\text{u,OPA}}_1, \cdots, \mathcal{P}^{\text{u,OPA}}_N\}} \ & P^{\text{u}}_{\text{elec}} \\ \text{s.t.} \ \ & \text{C3: } (11) \\ & \text{C4: } p^{\text{u}}_{i,f} \leq p^{\text{u}}_{\max} \\ & \text{C5: } p^{\text{u}}_{i,n} \leq p^{\text{u}}_{\max}. \end{aligned} \tag{15}$$

3) Optimal Solution: According to (10) and (11), given the channel gains, QoS requirements and noise power, the power requirements for the far and near users in the i-th user pair in both downlink and uplink channels are independent from each other. Hence, the optimal solutions for the above power minimization problems are that the far and near users in the i-th user pair in both downlink and uplink channels are allocated with minimum powers to satisfy their QoS requirements. Therefore, the closed-form OPA sets $\mathcal{P}^{b,\text{OPA}}_i = \{p^{b,\text{OPA}}_{i,f}, p^{b,\text{OPA}}_{i,n}\}$ with $b \in \{\text{d}, \text{u}\}$ can be obtained as follows:

$$\begin{cases} p^{\text{d,OPA}}_{i,f} = \mathbb{R}^{\text{d}}_{i,f} \left(\mathbb{R}^{\text{d}}_{i,n} \dfrac{P_z}{(h^{\text{d}}_{i,n})^2} + \dfrac{P_z}{(h^{\text{d}}_{i,f})^2} \right) \\ p^{\text{d,OPA}}_{i,n} = \mathbb{R}^{\text{d}}_{i,n} \dfrac{P_z}{(h^{\text{d}}_{i,n})^2} \end{cases}, \tag{16}$$

$$\begin{cases} p_{i,f}^{\mathrm{u,OPA}} = \mathbb{R}_{i,f}^{\mathrm{u}} \dfrac{P_z}{(h_{i,f}^{\mathrm{u}})^2} \\ p_{i,n}^{\mathrm{u,OPA}} = \mathbb{R}_{i,n}^{\mathrm{u}} (\mathbb{R}_{i,f}^{\mathrm{u}} + 1) \dfrac{P_z}{(h_{i,n}^{\mathrm{u}})^2} \end{cases}. \quad (17)$$

Although the optimal solution is obtained for a fixed target sum rate, it is generally applicable to dynamic LiFi-IoT systems with variable user QoS requirements. In practical applications, a central unit can be deployed to adaptively update the optimal solution according to the change of the channel information and QoS requirements of users.

According to (16) and (17), it is interesting to see that the minimum total electrical transmit powers in both downlink and uplink channels, i.e., $P_{\mathrm{elec,min}}^{b,\mathrm{OPA}}$ with $b \in \{\mathrm{d}, \mathrm{u}\}$, can be expressed by a unified formula which is given as follows:

$$P_{\mathrm{elec,min}}^{b,\mathrm{OPA}} = \sum_{i=1}^{N} \mathbb{R}_{i,f}^{b} \frac{P_z}{(h_{i,f}^{b})^2} + \mathbb{R}_{i,n}^{b} (\mathbb{R}_{i,f}^{b} + 1) \frac{P_z}{(h_{i,n}^{b})^2}, \quad (18)$$

and therefore, given the same rate requirements and channel conditions of each user pair, the required minimum total electrical transmit powers become exactly the same for both downlink and uplink channels. It should be noted that the QoS-guaranteed OPA strategy is obtained by assuming that the $2\ N$ users are divided into N pairs. Hence, efficient user pairing should be first performed before executing the QoS-guaranteed OPA strategy within each user pair.

E. User Pairing

As a typical IoT system usually consists of many users, i.e., IoT devices, it is efficient to divide these users into pairs[5] and a hybrid NOMA/OMA scheme can be adopted to support multiple user pairs. Specifically, NOMA is adopted for the two users within each user pair, while OMA is applied for different user pairs. Hence, user pairing plays an important role in NOMA-based systems [39]–[41]. In this subsection, three user pairing approaches are discussed to efficiently divide $2\ N$ users into N user pairs.

1) Channel-Based User Pairing: Channel-based user pairing is the most popular user pairing approach in NOMA-based systems [15], [22], [23]. The key to implement channel-based user pairing is to pair the two users which have more distinctive channel conditions. For the channel-based user pairing, the $2\ N$ users are sorted based on their channel gains in the ascending order:

$$h_1^b \leq \cdots \leq h_k^b \leq \cdots \leq h_{2N}^b, \quad (19)$$

where h_k^b with $b \in \{\mathrm{d}, \mathrm{u}\}$ is given in (2). After that, the sorted $2\ N$ users are divided into two groups: the first group $G_1^{b,\mathrm{c}}$ contains the first half of the sorted users starting from user 1 to user N, with the superscript "c" standing for channel-based user pairing; the second group $G_2^{b,\mathrm{c}}$ consists of the second half starting from user $N+1$ to user $2\ N$. Hence, user pairing can be performed in the following manner: $U_i^{b,\mathrm{c}} = \{G_1^{b,\mathrm{c}}(i), G_2^{b,\mathrm{c}}(i)\}$, i.e., the i-th user pair $U_i^{b,\mathrm{c}}$ contains both the i-th user in $G_1^{b,\mathrm{c}}$ and the i-th user in $G_2^{b,\mathrm{c}}$ with $i = 1, 2, \cdots, N$.

[5]Considering the computational complexity and time delay at the receiver side, it is generally assumed that only two users are multiplexed in the power domain [21].

Algorithm 1 Adaptive channel and QoS-based user pairing

Input: h_k^b, $\widetilde{R}_k^b$, P_z, $b \in \{\mathrm{d}, \mathrm{u}\}$, $k = 1, 2, \cdots, 2\ N$
Output: optimal user pair $U_i^{b,\mathrm{opt}}$, $i = 1, 2, \cdots, N$
Step 1: channel-based user pairing
Sort $\{h_k^b\}_{k=1,2,\cdots,2\ N}$ in ascending order
Divide the sorted users into $G_1^{b,\mathrm{c}}$ and $G_2^{b,\mathrm{c}}$
Obtain $U_i^{b,\mathrm{c}} = \{G_1^{b,\mathrm{c}}(i), G_2^{b,\mathrm{c}}(i)\}$, $i = 1, 2, \cdots, N$
Calculate $P_{\mathrm{elec,min}}^{b,\mathrm{c}}$ using $U_i^{b,\mathrm{c}}$ and (18)
Step 2: QoS-based user pairing
Sort $\{\widetilde{R}_k^b\}_{k=1,2,\cdots,2\ N}$ in descending order
Divide the sorted users into $G_1^{b,\mathrm{q}}$ and $G_2^{b,\mathrm{q}}$
Obtain $U_i^{b,\mathrm{q}} = \{G_1^{b,\mathrm{q}}(i), G_2^{b,\mathrm{q}}(i)\}$, $i = 1, 2, \cdots, N$
Calculate $P_{\mathrm{elec,min}}^{b,\mathrm{q}}$ using $U_i^{b,\mathrm{q}}$ and (18)
Step 3: adaptive selection
for $i = 1$ to N **do**
  if $P_{\mathrm{elec,min}}^{b,\mathrm{c}} \leq P_{\mathrm{elec,min}}^{b,\mathrm{q}}$ **then**
    $U_i^{b,\mathrm{opt}} = U_i^{b,\mathrm{c}}$
  else
    $U_i^{b,\mathrm{opt}} = U_i^{b,\mathrm{q}}$
  end if
end for

Nevertheless, the channel-based user pairing approach only takes the channel conditions of different users into account, while their specific QoS requirements are not considered.

2) QoS-Based User Pairing: In practical bidirectional LiFi-IoT systems, the supported users, i.e., IoT devices, might have their own distinctive QoS requirements in both downlink and uplink channels. Hence, the impact of users' QoS requirements should be considered when performing user pairing. For the QoS-based user pairing, all the $2\ N$ users are sorted based on their QoS requirements in the descending order:

$$\widetilde{R}_1^b \geq \cdots \geq \widetilde{R}_k^b \geq \cdots \geq \widetilde{R}_{2N}^b, \quad (20)$$

where $\widetilde{R}_k^b$ with $b \in \{\mathrm{d}, \mathrm{u}\}$ denotes the QoS requirement, i.e., rate requirement, of the k-th user. Similarly, the first half and the second half of the sorted $2\ N$ users can be divided into two groups which are respectively denoted as $G_1^{b,\mathrm{q}}$ and $G_2^{b,\mathrm{q}}$, with the superscript "q" standing for QoS-based user pairing. Hence, QoS-based user pairing can be given as follows: $U_i^{b,\mathrm{q}} = \{G_1^{b,\mathrm{q}}(i), G_2^{b,\mathrm{q}}(i)\}$ with $i = 1, 2, \cdots, N$.

3) Adaptive Channel and QoS-Based User Pairing: In both the channel-based and the QoS-based user pairing approaches, only a single factor (i.e., channel gain or QoS requirement) is considered for all the users. However, due to the randomness of channel gains caused by random users' locations and the randomness of users' QoS requirements, both channel gains and QoS requirements of users should be considered when putting them into pairs.

In the following, an adaptive channel and QoS-based user pairing approach is proposed, which takes both users' channel gains and QoS requirements into consideration. The detailed procedures to perform adaptive channel and QoS-based user pairing are summarized in Algorithm 1, which includes three steps. In the first step, channel-based user pairing is performed and the corresponding minimum power requirement $P_{\mathrm{elec,min}}^{b,\mathrm{c}}$

is calculated based on the obtained user pairs $U_i^{b,\mathrm{c}}$ and (18). In the second step, QoS-based user pairing is conducted and the corresponding minimum power requirement $P_{\mathrm{elec,min}}^{b,\mathrm{q}}$ is obtained by utilizing $U_i^{b,\mathrm{q}}$ and (18). In the third step, the user pairing approach which requires a lower minimum power is adaptively selected as the optimal one for the bidirectional LiFi-IoT system. Considering the randomness of users' locations and/or users' QoS requirements, the proposed adaptive user pairing approach is able to dynamically select the optimal one from the channel-based and the QoS-based user pairing approaches to achieve a lower minimum power consumption and hence a higher EE.

IV. Performance Analysis

To fairly evaluate the performance of the bidirectional LiFi-IoT system using various multiple access techniques, we here adopt EE and UOP as two metrics for performance evaluation, which are analyzed in the following.

A. Analysis of EE

1) EE Using NOMA With OPA: For the bidirectional LiFi-IoT system using NOMA with OPA, the target sum rate in the downlink/uplink channel is given by $R^b = \sum_{i=1}^{N} \widetilde{R}_{i,f}^b + \widetilde{R}_{i,n}^b$ with $b \in \{\mathrm{d},\mathrm{u}\}$ and the corresponding minimum total electrical transmit power requirement $P_{\mathrm{elec,min}}^{b,\mathrm{OPA}}$ is derived in (18). Hence, according to (9), the EE of both downlink and uplink channels using NOMA with OPA can be obtained by the following unified formula:

$$\eta_{\mathrm{OPA}}^b = \frac{\sum_{i=1}^{N} \widetilde{R}_{i,f}^b + \widetilde{R}_{i,n}^b}{\sum_{i=1}^{N} \mathbb{R}_{i,f}^b \frac{P_z}{(h_{i,f}^b)^2} + \mathbb{R}_{i,n}^b (\mathbb{R}_{i,f}^b + 1) \frac{P_z}{(h_{i,n}^b)^2}}. \quad (21)$$

2) EE Using NOMA With Channel-Based Power Allocation: To compare the performance of NOMA with OPA and conventional NOMA with channel-based power allocation, the following two typical channel-based power allocation strategies are considered: (i) GRPA [14] and (ii) NGDPA [18]. Letting $\alpha_i^b = \frac{p_{i,n}^{b,\mathrm{NOMA}}}{p_{i,f}^{b,\mathrm{NOMA}}}$ denote the power allocation ratio between the near user and the far user in the i-th user pair using NOMA with $b \in \{\mathrm{d},\mathrm{u}\}$, the power allocation ratio using GRPA and NGDPA can be expressed by

$$\alpha_i^b = \begin{cases} \left(\frac{h_{i,f}^b}{h_{i,n}^b}\right)^2, & \text{GRPA} \\ \frac{h_{i,n}^b - h_{i,f}^b}{h_{i,n}^b}, & \text{NGDPA} \end{cases}. \quad (22)$$

To satisfy the QoS requirements of both the far and near users in i-th user pair, the minimum required electrical transmit powers using NOMA with GRPA and NGDPA can be given by

$$(p_{i,f}^{b,\mathrm{NOMA}}, p_{i,n}^{b,\mathrm{NOMA}}) = \begin{cases} \left(p_{i,f}^{b,\mathrm{OPA}}, \alpha_i^b p_{i,f}^{b,\mathrm{OPA}}\right), & \alpha_i^b \geq \frac{p_{i,n}^{b,\mathrm{OPA}}}{p_{i,f}^{b,\mathrm{OPA}}} \\ \left(\frac{p_{i,n}^{\mathrm{d,OPA}}}{\alpha_i^b}, p_{i,n}^{b,\mathrm{OPA}}\right), & \alpha_i^b < \frac{p_{i,n}^{b,\mathrm{OPA}}}{p_{i,f}^{b,\mathrm{OPA}}} \end{cases}. \quad (23)$$

Using (23), the minimum total electrical transmit power using NOMA with GRPA and NGDPA can be obtained. It can be clearly observed that the minimum required electrical transmit power using NOMA with GRPA and NGDPA is always larger or equal to that using NOMA with OPA. Therefore, the EE using NOMA with GRPA and NGDPA is always lower or equal to that using NOMA with OPA in both downlink and uplink channel, which is omitted here for brevity.

3) EE Using OMA: For the bidirectional LiFi-IoT system using OMA techniques such as FDMA/OFDMA and TDMA, as shown in Fig. 2, the QoS requirements of different users are satisfied by allocating them with different frequency or time resources.

For the far and near users in the i-th user pair in both downlink and uplink channels using NOMA, the required rates to meet their QoS requirements are denoted by $\widetilde{R}_{i,f}^b$ and $\widetilde{R}_{i,n}^b$ with $b \in \{\mathrm{d},\mathrm{u}\}$, respectively. When OMA is applied, to achieve the same individual rates as using NOMA, the required rates for both the far and near users in the i-th user pair is given by $\widetilde{R}_i^{b,\mathrm{OMA}} = \widetilde{R}_{i,f}^b + \widetilde{R}_{i,n}^b$. Since the far and near users in the i-th user pair are not mutually interfered, their achievable rates can be calculated by

$$\begin{cases} R_{i,f}^{b,\mathrm{OMA}} = \frac{1}{2}\log_2\left(1 + \frac{(h_{i,f}^b)^2 p_{i,f}^{b,\mathrm{OMA}}}{P_z}\right) \\ R_{i,n}^{b,\mathrm{OMA}} = \frac{1}{2}\log_2\left(1 + \frac{(h_{i,n}^b)^2 p_{i,n}^{b,\mathrm{OMA}}}{P_z}\right) \end{cases}, \quad (24)$$

where $p_{i,f}^{b,\mathrm{OMA}}$ and $p_{i,n}^{b,\mathrm{OMA}}$ denote the electrical transmit powers allocated to the far and near users in the i-th user pair, respectively. By denoting $\mathcal{R}_i^b = 2^{2(\widetilde{R}_{i,f}^b + \widetilde{R}_{i,n}^b)} - 1$ with $b \in \{\mathrm{d},\mathrm{u}\}$, to ensure their QoS requirements, the following power requirements should be satisfied:

$$\begin{cases} p_{i,f}^{b,\mathrm{OMA}} \geq \mathcal{R}_i^b \frac{P_z}{(h_{i,f}^b)^2} \\ p_{i,n}^{b,\mathrm{OMA}} \geq \mathcal{R}_i^b \frac{P_z}{(h_{i,n}^b)^2} \end{cases}, \quad (25)$$

and the minimum required electrical transmit powers for the far and near users in the i-th user pair in the downlink/uplink channel can be given by

$$\begin{cases} p_{i,f}^{b,\mathrm{OMA,min}} = \mathcal{R}_i^b \frac{P_z}{(h_{i,f}^b)^2} \\ p_{i,n}^{b,\mathrm{OMA,min}} = \mathcal{R}_i^b \frac{P_z}{(h_{i,n}^b)^2} \end{cases}. \quad (26)$$

As a result, the required minimum total electrical transmit power in the downlink/uplink channel using OMA is obtained by

$$P_{\mathrm{elec,min}}^{b,\mathrm{OMA}} = \sum_{i=1}^{N} \mathcal{R}_i^b \frac{P_z}{(h_{i,f}^b)^2} + \mathcal{R}_i^b \frac{P_z}{(h_{i,n}^b)^2}, \quad (27)$$

and the EE of the downlink/uplink channel using OMA is given as follows:

$$\eta_{\mathrm{OMA}}^b = \frac{\sum_{i=1}^{N} \widetilde{R}_{i,f}^b + \widetilde{R}_{i,n}^b}{\sum_{i=1}^{N} \mathcal{R}_i^b \frac{P_z}{(h_{i,f}^b)^2} + \mathcal{R}_i^b \frac{P_z}{(h_{i,n}^b)^2}}. \quad (28)$$

Based on the derived EE of the downlink/uplink channel in the bidirectional LiFi-IoT system using NOMA with OPA

Algorithm 2 Calculation of downlink UOP $P_{\text{out}}^{\text{d}}$

Input: h_k^{d}, $\widetilde{R}_k^{\text{d}}$, P_z, $P_{\max}^{\text{d}}$, $k = 1, 2, \cdots, 2\ N$
Output: $P_{\text{out}}^{\text{d}}$
Initialize $k_{\text{out}}^{\text{d}} = 0$
Calculate $p_{i,f}^{\text{d,OPA}}$ and $p_{i,n}^{\text{d,OPA}}$ using (16), $i = 1, 2, \cdots, N$
Sort $\{p_{i,f}^{\text{d,OPA}}, p_{i,n}^{\text{d,OPA}}\}_{i=1,2,\cdots,N}$ in descending order
Obtain the sorted powers $\{p_k^{\text{d}}\}_{k=1,2,\cdots,2\ N}$
for $k = 1$ to $2\ N$ **do**
  Calculate $P_k^{\text{d}} = \sum_{j=k}^{2\ N} p_k^{\text{d}}$
  if $P_k^{\text{d}} > P_{\max}^{\text{d}}$ **then**
    $k_{\text{out}}^{\text{d}} = k_{\text{out}}^{\text{d}} + 1$
  end if
end for
Calculate $P_{\text{out}}^{\text{d}} = \frac{k_{\text{out}}^{\text{d}}}{2\ N}$

and OMA, as given by (21) and (28), we have the following proposition.

Proposition 2: The EE of the downlink/uplink channel in the bidirectional LiFi-IoT system using NOMA with OPA is always larger or equal to that using OMA, i.e., $\eta_{\text{OPA}}^{b} \geq \eta_{\text{OMA}}^{b}$, when $\widetilde{R}_{i,f}^{b}, \widetilde{R}_{i,n}^{b}, \geq 0$ (bit/s/Hz).

Proof: Please refer to the appendix. ∎

Proposition 2 demonstrates that NOMA with OPA is more energy-efficient than OMA, which is very suitable for energy-sensitive IoT applications.

B. Analysis of UOP

Considering the maximum total downlink electrical transmit power constraint at the LiFi AP and the maximum uplink electrical transmit power constraint at each user, user outage might occur in both downlink and uplink channels of the bidirectional LiFi-IoT system. To evaluate the outage performance of the system, UOP is adopted as the metric in the following analysis.

For the downlink channel, the minimum required total electrical transmit power using NOMA with OPA is given by

$$P_{\text{elec,min}}^{\text{d,OPA}} = \sum_{i=1}^{N} \mathbb{R}_{i,f}^{\text{d}} \frac{P_z}{(h_{i,f}^{\text{d}})^2} + \mathbb{R}_{i,n}^{\text{d}} (\mathbb{R}_{i,f}^{\text{d}} + 1) \frac{P_z}{(h_{i,n}^{\text{d}})^2}. \quad (29)$$

Due to the maximum total downlink electrical transmit power constraint at the LiFi AP, $P_{\text{elec,min}}^{\text{d,OPA}}$ cannot exceed its maximum value $P_{\max}^{\text{d}}$. If $P_{\text{elec,min}}^{\text{d,OPA}}$ exceeds $P_{\max}^{\text{d}}$, the LiFi AP will fail to support all the downlink users. Hence, the LiFi AP can only connect with a selected subset of the downlink users so as to meet the maximum total downlink electrical transmit power constraint. With the goal to let the LiFi AP connect with more downlink users, it is reasonable to exclude the users which require the highest powers outside the subset.

Let $k_{\text{out}}^{\text{d}}$ denote the number of downlink users that cannot connect with the LiFi AP, the downlink UOP can be calculated by $P_{\text{out}}^{\text{d}} = \frac{k_{\text{out}}^{\text{d}}}{2\ N}$. The detailed procedures to calculate $P_{\text{out}}^{\text{d}}$ are given in Algorithm 2. Due to the randomness of both users' locations and QoS requirements, $P_{\text{out}}^{\text{d}}$ is calculated for multiple times so as to obtain a stable average value. For the uplink channel, the electrical transmit power of each user should not exceed the maximum value $p_{\max}^{\text{u}}$. The calculation of the uplink UOP $P_{\text{out}}^{\text{u}}$ is hence straightforward. We only need to count the number of uplink users which require a minimum electrical transmit power higher than $p_{\max}^{\text{u}}$, i.e., $k_{\text{out}}^{\text{u}}$, and $P_{\text{out}}^{\text{u}} = \frac{k_{\text{out}}^{\text{u}}}{2\ N}$. Similarly, $P_{\text{out}}^{\text{u}}$ is calculated for multiple times to yield a stable average value.

Following the similar manner, both downlink and uplink UOPs using NOMA with channel-based power allocation and OMA can also be achieved, which are omitted here for brevity.

TABLE I
SIMULATION PARAMETERS

Parameter name, notation	Value
Maximum vertical distance, $l_{\max}$	2.5 m
Minimum vertical distance, $l_{\min}$	1.5 m
Maximum horizontal distance, $r_{\max}$	3 m
Minimum horizontal distance, $r_{\min}$	0 m
Visible/infrared light LED semi-angle, Ψ	70°
Visible/infrared light LED conversion efficiency, β	1 W/A
Visible/infrared light PD responsivity, ρ	0.4 A/W
Visible/infrared light PD active area, A	1 cm^2
Receiver half-angle FOV, Φ	70°
Optical filter gain, g_f	0.9
Optical concentrator refractive index, n	1.5
Overall system bandwidth, B_s	20 MHz
Noise PSD, N_0	10^{-22} A^2/Hz

V. PERFORMANCE EVALUATION AND COMPARISON

A. Simulation Setup

In order to substantiate our derived analytical results, extensive Monte Carlo simulations are performed. If not otherwise specified, the simulation parameters of the considered single-cell bidirectional LiFi-IoT system are listed in Table I. For the purpose of performance comparison, four multiple access techniques are considered including: (i) OMA, (ii) NOMA with GRPA, (iii) NOMA with NGDPA and (iv) NOMA with OPA. Moreover, three user pairing approaches as discussed in Section III.E are evaluated which includes: (i) channel-based user pairing, (ii) QoS-based user pairing and (iii) adaptive channel and QoS-based user pairing. In the following evaluation, we assume that perfect channel state information (CSI) of all the users is available when performing user pairing and power allocation in the bidirectional LiFi-IoT system. For simplicity and without loss of generality, we assume that the overall system bandwidth for both downlink and uplink channels are the same (i.e., $B_{\text{elec}}^{\text{d}} = B_{\text{elec}}^{\text{u}} = B_s$) and equal bandwidth allocation[6] is considered for different user pairs (i.e., $B_i^{\text{d}} = B_i^{\text{u}} = \frac{B_s}{N}$ for $i = 1, 2, \cdots, N$).

B. Results and Discussions

In the subsection, we present analytical and simulation results to evaluate and compare the performance of the considered single-cell bidirectional LiFi-IoT system using different multiple access techniques. Without loss of generality, we here assume that the vertical and horizontal distances of all the users are uniformly distributed between 1.5 to 2.5 m and 0 to

[6]As a simple but effective bandwidth allocation approach, equal bandwidth allocation has been considered in most hybrid NOMA/OMA systems [22], [23].

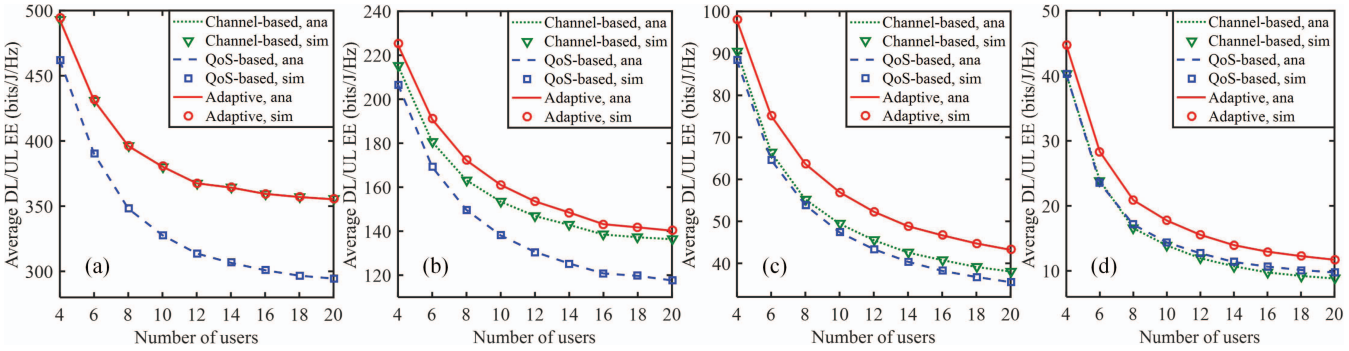

Fig. 4. Average downlink/uplink (DL/UL) EE vs. the number of users using NOMA with OPA with different user pairing approaches for (a) $\widetilde{R} = 1$, (b) $\widetilde{R} = \{1, 2\}$, (c) $\widetilde{R} = \{1, 2, 3\}$ and (d) $\widetilde{R} = \{1, 2, 3, 4\}$.

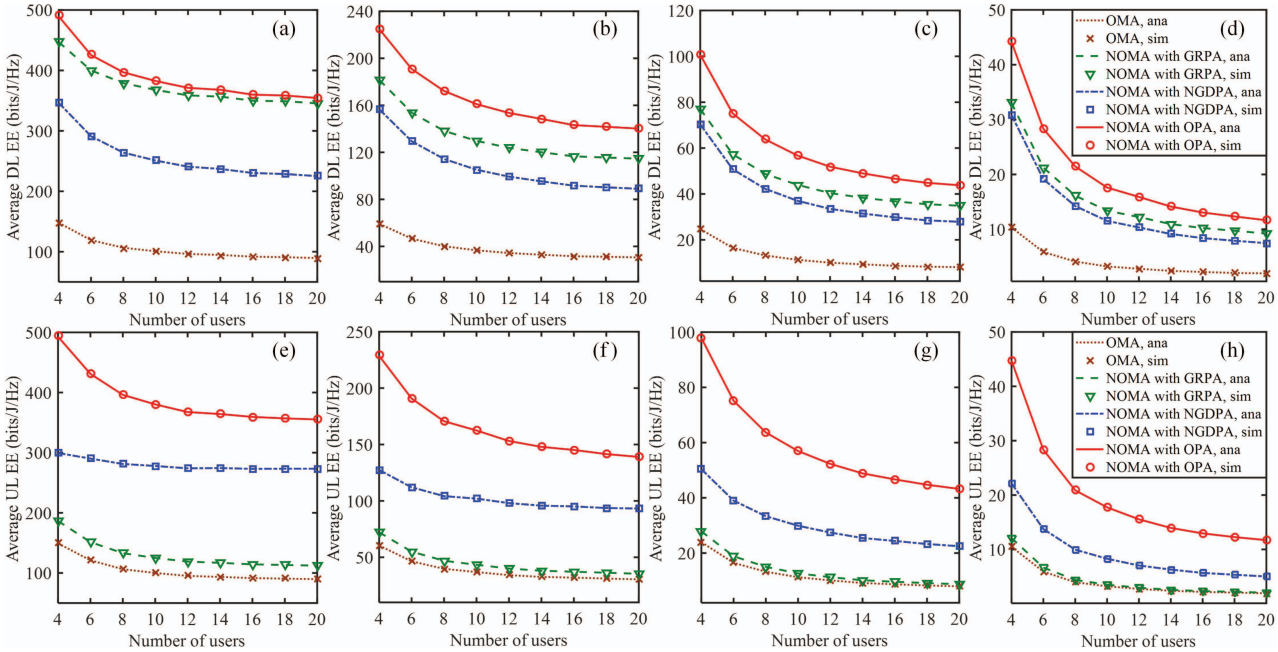

Fig. 5. Average downlink (DL) EE vs. the number of users using different multiple access techniques with adaptive channel and QoS-based user paring for (a) $\widetilde{R} = 1$, (b) $\widetilde{R} = \{1, 2\}$, (c) $\widetilde{R} = \{1, 2, 3\}$ and (d) $\widetilde{R} = \{1, 2, 3, 4\}$, and average uplink (UL) EE vs. the number of users using different multiple access techniques with adaptive channel and QoS-based user paring for (e) $\widetilde{R} = 1$, (f) $\widetilde{R} = \{1, 2\}$, (g) $\widetilde{R} = \{1, 2, 3\}$ and (h) $\widetilde{R} = \{1, 2, 3, 4\}$.

3 m, respectively. Moreover, we define $\widetilde{R}$ as the given QoS set for both downlink and uplink channels, where the elements of $\widetilde{R}$ have a unit of bits/s/Hz. Both the downlink and uplink QoS requirements of the users are randomly selected from the given QoS set $\widetilde{R}$. In order to obtain stable performance metrics, including EE and UOP, under random user locations and QoS requirements, we calculate the average EE and UOP over totally 10000 independent trials.

We first evaluate the average EE versus the number of users using NOMA with OPA in the bidirectional LiFi-IoT system. Since the EE of both downlink and uplink channels using NOMA with OPA can be expressed by a unified formula as in (21), the obtained average downlink EE and uplink EE become nearly the same after 10000 independent trials. Figs. 4(a)-(d) depict the average downlink/uplink EE versus the number of users using NOMA with OPA with different user pairing approaches under various given QoS sets. When $\widetilde{R} = 1$, as shown in Fig. 4(a), the average EE decreases with the increase of users for all the three user pairing approaches. Moreover, the channel-based user paring approach and the adaptive channel and QoS-based user paring approach obtain the same average EE, and both greatly outperform the QoS-based user paring approach. This is because the QoS requirements of all the user are the same, and hence random user pairing is achieved when sorting the users according to their QoS requirements. However, when diverse QoS requirements are desired by the users, the adaptive approach achieves higher average EE than the channel-based approach, as can be seen from Figs. 4(b), (c) and (d). More specifically, when $\widetilde{R} = \{1, 2, 3, 4\}$, the QoS-based user paring approach outperforms the channel-based approach, especially for a relatively large number of users. It can be found from Figs. 4(a)-(d) that it is beneficial to consider the impact of users' QoS requirements when performing user pairing and the proposed adaptive approach can be an efficient user pairing approach for energy-efficient bidirectional LiFi-IoT systems. It can also be seen from Fig. 4 that the simulation results agree well with the analytical results.

In the next, we compare the average downlink EE of four different multiple access techniques utilizing adaptive channel

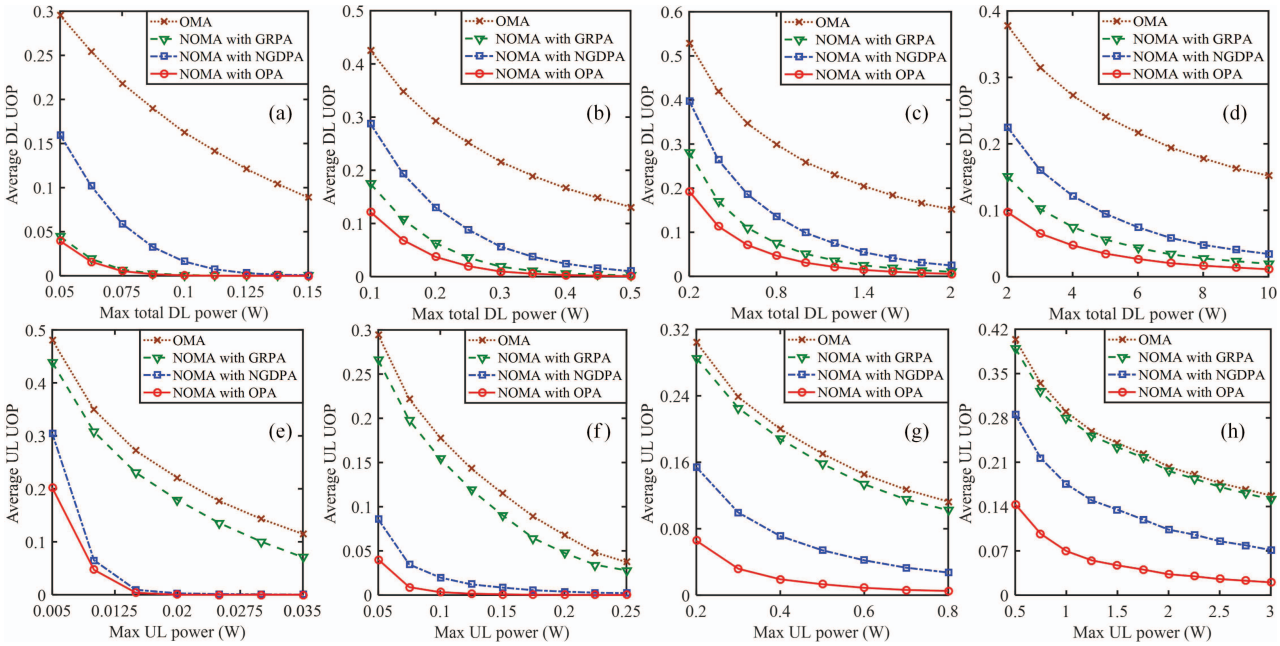

Fig. 6. Average downlink (DL) UOP vs. the maximum total DL power using different multiple access techniques with adaptive channel and QoS-based user paring for (a) $\widetilde{R}=1$, (b) $\widetilde{R}=\{1,2\}$, (c) $\widetilde{R}=\{1,2,3\}$ and (d) $\widetilde{R}=\{1,2,3,4\}$, and average uplink (UL) UOP vs. the maximum UL power using different multiple access techniques with adaptive channel and QoS-based user paring for (e) $\widetilde{R}=1$, (f) $\widetilde{R}=\{1,2\}$, (g) $\widetilde{R}=\{1,2,3\}$ and (h) $\widetilde{R}=\{1,2,3,4\}$.

and QoS-based user paring under various given QoS sets, as shwon in Figs. 5(a)-(d). As we can see, OMA always achieves the lowest average downlink EE, while NOMA with NGDPA outperforms OMA. NOMA with GRPA is shown to be more energy-saving than NOMA with NGDPA, especially when users' downlink QoS requirements are less diverse. Nevertheless, NOMA with OPA is proven to be the most energy-efficient one among all the four techniques, which achieves greatly improved average downlink EE than NOMA with GRPA when users have diverse downlink QoS requirements. Figs. 5(e)-(h) show the average uplink EE of four different multiple access techniques using adaptive channel and QoS-based user paring under various given QoS sets. It can be seen that the lowest average uplink EE is obtained by OMA, while NOMA with NGDPA outperforms NOMA with GRPA in the uplink. Furthermore, NOMA with OPA achieves a significant average uplink EE improvement in comparison to NOMA with NGDPA, regardless of the number of users and the diversity of users' QoS requirements.

Figs. 6(a)-(d) show the average downlink UOP versus the maximum total downlink power using different multiple access techniques with adaptive channel and QoS-based user paring under various given QoS sets. It can be seen that OMA always obtains the highest average downlink UOP among all the four multiple access techniques. Moreover, NOMA with GRPA is shown to be more superior than NOMA with NGDPA in terms of average downlink UOP, especially for less diverse user QoS requirements. Among them, NOMA with OPA achieves the lowest average downlink UOP regardless of the maximum total downlink power and the diversity of users' QoS requirements. Figs. 6(e)-(h) depict the average uplink UOP versus the maximum uplink power using NOMA with OPA using different user pairing approaches under various given QoS sets. It is shown that OMA performs the worst while NOMA with OPA performs the best among all the four multiple access techniques. Moreover, NOMA with GRPA slightly outperforms OMA, while NOMA with NGDPA greatly outperforms NOMA with GRPA and it achieves comparable average uplink UOP as NOMA with OPA for $\widetilde{R}=1$. When more diverse QoS requirements are desired by users, NOMA with OPA gradually outperforms NOMA with NGDPA. Fig. 6 demonstrates that NOMA with OPA is more efficient than OMA and NOMA with GRPA/NGDPA to satisfactorily support multiple users in both downlink and uplink channels.

VI. Conclusion

In this paper, we have proposed an energy-efficient NOMA technique for bidirectional LiFi-IoT communication, which adopts a QoS-guaranteed OPA strategy to maximize the EE of both downlink and uplink channels. We have identified and proved the optimal decoding orders in both downlink and uplink channels, and derived closed-form OPA sets. We have further proposed an adaptive channel and QoS-based user pairing approach which considers both users' channel gains and QoS requirements. The EE and UOP performance of the bidirectional LiFi-IoT system using different multiple access techniques has also been analyzed. Extensive analytical and simulation results show that, compared with OMA and conventional NOMA techniques, the proposed NOMA adopting OPA with adaptive channel and QoS-based user pairing can significantly improve both the EE and UOP performance of the bidirectional LiFi-IoT system.

Appendix

A. Proof of Theorem 1

With the decoding order $\mathbb{O}^{\mathrm{d}}_{i,\mathrm{high}} \geq \mathbb{O}^{\mathrm{d}}_{i,\mathrm{low}}$, the high priority user decodes its message signal directly by treating the intended message signal for the low priority user as

interference, while the low priority user needs to decode the intended message signal for the high priority user and apply SIC to decode its own message signal. Hence, the achievable rates of the high and low priority users in the i-th user pair can be given by

$$\begin{cases} R^{\mathrm{d}}_{i,\mathrm{high}} = \frac{1}{2}\log_2\left(1+\frac{(h^{\mathrm{d}}_{i,\mathrm{high}})^2 p^{\mathrm{d}}_{i,\mathrm{high}}}{(h^{\mathrm{d}}_{i,\mathrm{high}})^2 p^{\mathrm{d}}_{i,\mathrm{low}}+P_z}\right) \\ R^{\mathrm{d}}_{i,\mathrm{low}} = \frac{1}{2}\log_2\left(1+\frac{(h^{\mathrm{d}}_{i,\mathrm{low}})^2 p^{\mathrm{d}}_{i,\mathrm{low}}}{P_z}\right) \end{cases}, \quad (30)$$

where the scaling factor $\frac{1}{2}$ is due to the Hermitian symmetry [15]. Note that (30) is obtained under the condition that perfect SIC can be performed for the low priority user. As discussed in [15], perfect SIC can be achieved when the low priority user can successfully decode the message intended for the high priority user, i.e., the achievable rate for the low priority user to decode the high priority user's message signal should be equal or higher than the rate requirement of the high priority user. Accordingly, the achievable rate for the low priority user to decode the high priority user's message signal is given by

$$R^{\mathrm{d}}_{i,\mathrm{low}\to\mathrm{high}} = \frac{1}{2}\log_2\left(1+\frac{(h^{\mathrm{d}}_{i,\mathrm{low}})^2 p^{\mathrm{d}}_{i,\mathrm{high}}}{(h^{\mathrm{d}}_{i,\mathrm{low}})^2 p^{\mathrm{d}}_{i,\mathrm{low}}+P_z}\right). \quad (31)$$

Hence, to meet the rate requirements of both the high priority user and the low priority user with perfect SIC in the i-th user pair, the following conditions need to be satisfied:

$$\begin{cases} \min\{R^{\mathrm{d}}_{i,\mathrm{high}}, R^{\mathrm{d}}_{i,\mathrm{low}\to i,\mathrm{high}}\} \geq \widetilde{R}^{\mathrm{d}}_{i,\mathrm{high}} \\ R^{\mathrm{d}}_{i,\mathrm{low}} \geq \widetilde{R}^{\mathrm{d}}_{i,\mathrm{low}} \end{cases}. \quad (32)$$

By denoting $\mathbb{R}^{\mathrm{d}}_{i,\mathrm{high}} = 2^{2\widetilde{R}^{\mathrm{d}}_{i,\mathrm{high}}}-1$, $\mathbb{R}^{\mathrm{d}}_{i,\mathrm{low}} = 2^{2\widetilde{R}^{\mathrm{d}}_{i,\mathrm{low}}}-1$ and $h^{\mathrm{d}}_{i,\mathrm{min}} = \min\{h^{\mathrm{d}}_{i,\mathrm{high}}, h^{\mathrm{d}}_{i,\mathrm{low}}\}$, according to (32), we can obtain the power requirements of two users as follows:

$$\begin{cases} p^{\mathrm{d}}_{i,\mathrm{high}} \geq \mathbb{R}^{\mathrm{d}}_{i,\mathrm{high}}\left(p^{\mathrm{d}}_{i,\mathrm{low}}+\frac{P_z}{(h^{\mathrm{d}}_{i,\mathrm{min}})^2}\right) \\ p^{\mathrm{d}}_{i,\mathrm{low}} \geq \mathbb{R}^{\mathrm{d}}_{i,\mathrm{low}}\frac{P_z}{(h^{\mathrm{d}}_{i,\mathrm{low}})^2} \end{cases}. \quad (33)$$

By observing (33), we can easily rewrite it into (5). Therefore, *Theorem 1* is proved. ■

B. Proof of Theorem 2

Based on the decoding order $\mathbb{O}^{\mathrm{u}}_{i,\mathrm{high}} \geq \mathbb{O}^{\mathrm{u}}_{i,\mathrm{low}}$, (7) can be rewritten as:

$$y^{\mathrm{u}}_i = h^{\mathrm{u}}_{i,\mathrm{high}}\sqrt{p^{\mathrm{u}}_{i,\mathrm{high}}}s^{\mathrm{u}}_{i,\mathrm{high}} + h^{\mathrm{u}}_{i,\mathrm{low}}\sqrt{p^{\mathrm{u}}_{i,\mathrm{low}}}s^{\mathrm{u}}_{i,\mathrm{low}} + z^{\mathrm{u}}_i. \quad (34)$$

Hence, the LiFi AP first decodes the high priority user's message signal directly by treating the low priority user's message signal, and then decodes the low priority user's message signal after applying SIC to remove the high priority user's message signal. Hence, the achievable rates of the high and low priority users in i-th user pair are obtained as follows:

$$\begin{cases} R^{\mathrm{u}}_{i,\mathrm{high}} = \frac{1}{2}\log_2\left(1+\frac{(h^{\mathrm{u}}_{i,\mathrm{high}})^2 p^{\mathrm{u}}_{i,\mathrm{high}}}{(h^{\mathrm{u}}_{i,\mathrm{low}})^2 p^{\mathrm{u}}_{i,\mathrm{low}}+P_z}\right) \\ R^{\mathrm{u}}_{i,\mathrm{low}} = \frac{1}{2}\log_2\left(1+\frac{(h^{\mathrm{u}}_{i,\mathrm{low}})^2 p^{\mathrm{u}}_{i,\mathrm{low}}}{P_z}\right) \end{cases}. \quad (35)$$

To meet the QoS requirements for the LiFi AP to successfully decode the intended message signals for both the high and low priority users in i-th user pair, the following conditions need to be satisfied:

$$\begin{cases} R^{\mathrm{u}}_{i,\mathrm{high}} \geq \widetilde{R}^{\mathrm{u}}_{i,\mathrm{high}} \\ R^{\mathrm{u}}_{i,\mathrm{low}} \geq \widetilde{R}^{\mathrm{u}}_{i,\mathrm{low}} \end{cases}. \quad (36)$$

By denoting $\mathbb{R}^{\mathrm{u}}_{i,\mathrm{high}} = 2^{2\widetilde{R}^{\mathrm{u}}_{i,\mathrm{high}}}-1$ and $\mathbb{R}^{\mathrm{u}}_{i,\mathrm{low}} = 2^{2\widetilde{R}^{\mathrm{u}}_{i,\mathrm{low}}}-1$, according to (36), we can have the power requirements of the high and low priority users in i-th user pair:

$$\begin{cases} p^{\mathrm{u}}_{i,\mathrm{high}} \geq \mathbb{R}^{\mathrm{u}}_{i,\mathrm{high}}\frac{(h^{\mathrm{u}}_{i,\mathrm{low}})^2\ p^{\mathrm{u}}_{i,\mathrm{low}}+P_z}{(h^{\mathrm{u}}_{i,\mathrm{high}})^2} \\ p^{\mathrm{u}}_{i,\mathrm{low}} \geq \mathbb{R}^{\mathrm{u}}_{i,\mathrm{low}}\frac{P_z}{(h^{\mathrm{u}}_{i,\mathrm{low}})^2} \end{cases}. \quad (37)$$

Substituting $(h^{\mathrm{u}}_{i,\mathrm{low}})^2\ p^{\mathrm{u}}_{i,\mathrm{low}}+P_z \geq (\mathbb{R}^{\mathrm{u}}_{i,\mathrm{low}}+1)\ P_z$ into (37) yields (8). Hence, the proof of *Theorem 2* is completed. ■

C. Proof of Proposition 1

Since there are only two users in the i-th user pair, the decoding orders for both downlink and uplink channels can only have two options: i.e., $\mathbb{O}^{\mathrm{d}}_{i,f} \geq \mathbb{O}^{\mathrm{d}}_{i,n}$ and $\mathbb{O}^{\mathrm{d}}_{i,f} < \mathbb{O}^{\mathrm{d}}_{i,n}$ for downlink, and $\mathbb{O}^{\mathrm{u}}_{i,f} \geq \mathbb{O}^{\mathrm{u}}_{i,n}$ and $\mathbb{O}^{\mathrm{u}}_{i,f} < \mathbb{O}^{\mathrm{u}}_{i,n}$ for uplink.

For the downlink with $\mathbb{O}^{\mathrm{d}}_{i,f} \geq \mathbb{O}^{\mathrm{d}}_{i,n}$, using (5), the power requirements can be obtained by

$$\begin{cases} p^{\mathrm{d}}_{i,f} \geq \mathbb{R}^{\mathrm{d}}_{i,f}\left(\mathbb{R}^{\mathrm{d}}_{i,n}\frac{P_z}{(h^{\mathrm{d}}_{i,n})^2}+\frac{P_z}{(h^{\mathrm{d}}_{i,\mathrm{min}})^2}\right) \\ p^{\mathrm{d}}_{i,n} \geq \mathbb{R}^{\mathrm{d}}_{i,n}\frac{P_z}{(h^{\mathrm{d}}_{i,n})^2} \end{cases}, \quad (38)$$

where $h^{\mathrm{d}}_{i,\mathrm{min}} = h^{\mathrm{d}}_{i,f}$. Hence, the total required power of both the far and near users in the i-th user pair in the downlink with $\mathbb{O}^{\mathrm{d}}_{i,f} \geq \mathbb{O}^{\mathrm{d}}_{i,n}$ is obtained by

$$\begin{aligned} p^{\mathrm{d}}_i = p^{\mathrm{d}}_{i,f} + p^{\mathrm{d}}_{i,n} &\geq \mathbb{R}^{\mathrm{d}}_{i,f}\mathbb{R}^{\mathrm{d}}_{i,n}\frac{P_z}{(h^{\mathrm{d}}_{i,n})^2} \\ &+\mathbb{R}^{\mathrm{d}}_{i,f}\frac{P_z}{(h^{\mathrm{d}}_{i,f})^2} + \mathbb{R}^{\mathrm{d}}_{i,n}\frac{P_z}{(h^{\mathrm{d}}_{i,n})^2}. \end{aligned} \quad (39)$$

Similarly, the total required power of both the far and near users in the i-th user pair in the downlink with $\mathbb{O}^{\mathrm{d}}_{i,f} < \mathbb{O}^{\mathrm{d}}_{i,n}$ can also be achieved by

$$p^{\mathrm{d},\dagger}_i \geq \mathbb{R}^{\mathrm{d}}_{i,f}\mathbb{R}^{\mathrm{d}}_{i,n}\frac{P_z}{(h^{\mathrm{d}}_{i,f})^2} + \mathbb{R}^{\mathrm{d}}_{i,f}\frac{P_z}{(h^{\mathrm{d}}_{i,f})^2} + \mathbb{R}^{\mathrm{d}}_{i,n}\frac{P_z}{(h^{\mathrm{d}}_{i,f})^2}. \quad (40)$$

Since $h^{\mathrm{d}}_{i,f} \leq h^{\mathrm{d}}_{i,n}$, by observing (39) and (40), we can find that the minimum power requirement with $\mathbb{O}^{\mathrm{d}}_{i,f} < \mathbb{O}^{\mathrm{d}}_{i,n}$ is larger or equal to that with $\mathbb{O}^{\mathrm{d}}_{i,f} \geq \mathbb{O}^{\mathrm{d}}_{i,n}$. As a result, $\mathbb{O}^{\mathrm{d}}_{i,f} \geq \mathbb{O}^{\mathrm{d}}_{i,n}$ is the optimal decoding order for the downlink.

Next, for the uplink with $\mathbb{O}^{\mathrm{u}}_{i,f} \geq \mathbb{O}^{\mathrm{u}}_{i,n}$, using (8), the power requirements can be achieved by

$$\begin{cases} p^{\mathrm{u}}_{i,f} \geq \mathbb{R}^{\mathrm{u}}_{i,f}(\mathbb{R}^{\mathrm{u}}_{i,n}+1)\frac{P_z}{(h^{\mathrm{u}}_{i,f})^2} \\ p^{\mathrm{u}}_{i,n} \geq \mathbb{R}^{\mathrm{u}}_{i,n}\frac{P_z}{(h^{\mathrm{u}}_{i,n})^2} \end{cases}, \quad (41)$$

$$P_{\text{elec,min}}^{b,\text{OMA}} - P_{\text{elec,min}}^{b,\text{OPA}} = \sum_{i=1}^{N} 2^{2\widetilde{R}_{i,f}^{b}} \left(2^{2\widetilde{R}_{i,n}^{b}} - 1\right) \frac{P_z}{(h_{i,f}^{b})^2} + \left(2^{2\widetilde{R}_{i,f}^{b}} - 1\right) \frac{P_z}{(h_{i,n}^{b})^2}. \tag{44}$$

and the total required power of both the far and near users in the i-th user pair in the uplink with $\mathbb{O}_{i,f}^{\text{u}} \geq \mathbb{O}_{i,n}^{\text{u}}$ is given by

$$p_i^{\text{u}} = p_{i,f}^{\text{u}} + p_{i,n}^{\text{u}} \geq \mathbb{R}_{i,f}^{\text{u}} \mathbb{R}_{i,n}^{\text{u}} \frac{P_z}{(h_{i,f}^{\text{u}})^2} + \mathbb{R}_{i,f}^{\text{u}} \frac{P_z}{(h_{i,f}^{\text{u}})^2} + \mathbb{R}_{i,n}^{\text{u}} \frac{P_z}{(h_{i,n}^{\text{u}})^2}. \tag{42}$$

Similarly, we can also obtain the total power requirement of both the far and near users in the i-th user pair in the uplink with $\mathbb{O}_{i,f}^{\text{u}} < \mathbb{O}_{i,n}^{\text{u}}$ as follows:

$$p_i^{\text{u},\dagger} \geq \mathbb{R}_{i,f}^{\text{u}} \mathbb{R}_{i,n}^{\text{u}} \frac{P_z}{(h_{i,n}^{\text{u}})^2} + \mathbb{R}_{i,f}^{\text{u}} \frac{P_z}{(h_{i,f}^{\text{u}})^2} + \mathbb{R}_{i,n}^{\text{u}} \frac{P_z}{(h_{i,n}^{\text{u}})^2}. \tag{43}$$

Using $h_{i,f}^{\text{u}} \leq h_{i,n}^{\text{u}}$ and observing (42) and (43), it can be seen that the minimum power requirement with $\mathbb{O}_{i,f}^{\text{u}} \geq \mathbb{O}_{i,n}^{\text{u}}$ is larger or equal to that with $\mathbb{O}_{i,f}^{\text{u}} < \mathbb{O}_{i,n}^{\text{u}}$. Hence, $\mathbb{O}_{i,f}^{\text{u}} < \mathbb{O}_{i,n}^{\text{u}}$ is the optimal decoding order for the uplink. Therefore, *Proposition 1* is proved. ■

D. Proof of Proposition 2

By observing (21) and (28), to prove that $\eta_{\text{OPA}}^{b} \geq \eta_{\text{OMA}}^{b}$, we only need to prove $P_{\text{elec,min}}^{b,\text{OPA}} \leq P_{\text{elec,min}}^{b,\text{OMA}}$. Using (18) and (27), the difference between $P_{\text{elec,min}}^{b,\text{OMA}}$ and $P_{\text{elec,min}}^{b,\text{OPA}}$ can be given by (44), as shown on the top of the page.

Due to $\widetilde{R}_{i,f}^{b}, \widetilde{R}_{i,n}^{b} \geq 0$, we have $2^{2\widetilde{R}_{i,f}^{b}}, 2^{2\widetilde{R}_{i,n}^{b}} \geq 1$ and hence we can obtain $P_{\text{elec,min}}^{b,\text{OMA}} - P_{\text{elec,min}}^{b,\text{OPA}} \geq 0$, i.e., $P_{\text{elec,min}}^{b,\text{OPA}} \leq P_{\text{elec,min}}^{b,\text{OMA}}$. Therefore, the proof of *Proposition 2* is completed. ■

REFERENCES

[1] L. Atzori, A. Iera, and G. Morabito, "The Internet of Things: A survey," *Comput. Netw.*, vol. 54, no. 15, pp. 2787–2805, Oct. 2010.

[2] L. Da Xu, W. He, and S. Li, "Internet of Things in industries: A survey," *IEEE Trans. Ind. Informat.*, vol. 10, no. 4, pp. 2233–2243, Nov. 2014.

[3] M. R. Palattella *et al.*, "Internet of Things in the 5G era: Enablers, architecture, and business models," *IEEE J. Sel. Areas Commun.*, vol. 34, no. 3, pp. 510–527, Mar. 2016.

[4] I. Demirkol, D. Camps-Mur, J. Paradells, M. Combalia, W. Popoola, and H. Haas, "Powering the Internet of Things through light communication," *IEEE Commun. Mag.*, vol. 57, no. 6, pp. 107–113, Jun. 2019.

[5] H. Haas, L. Yin, Y. Wang, and C. Chen, "What is LiFi?" *J. Lightw. Technol.*, vol. 34, no. 6, pp. 1533–1544, Mar. 15, 2016.

[6] T. Komine and M. Nakagawa, "Fundamental analysis for visible-light communication system using LED lights," *IEEE Trans. Consum. Electron.*, vol. 50, no. 1, pp. 100–107, Feb. 2004.

[7] H. Burchardt, N. Serafimovski, D. Tsonev, S. Videv, and H. Haas, "VLC: Beyond point-to-point communication," *IEEE Commun. Mag.*, vol. 52, no. 7, pp. 98–105, Jul. 2014.

[8] L. I. Albraheem, L. H. Alhudaithy, A. A. Aljaser, M. R. Aldhafian, and G. M. Bahliwah, "Toward designing a Li-Fi-based hierarchical IoT architecture," *IEEE Access*, vol. 6, pp. 40811–40825, 2018.

[9] P. D. Diamantoulakis and G. K. Karagiannidis, "Simultaneous lightwave information and power transfer (SLIPT) for indoor IoT applications," in *Proc. IEEE Global Commun. Conf. (GLOBECOM)*, Dec. 2017, pp. 1–6.

[10] P. K. Sharma, Y.-S. Jeong, and J. H. Park, "EH-HL: Effective communication model by integrated EH-WSN and hybrid LiFi/WiFi for IoT," *IEEE Internet Things J.*, vol. 5, no. 3, pp. 1719–1726, Jun. 2018.

[11] A. M. Abdelhady, O. Amin, A. Chaaban, B. Shihada, and M.-S. Alouini, "Downlink resource allocation for dynamic TDMA-based VLC systems," *IEEE Trans. Wireless Commun.*, vol. 18, no. 1, pp. 108–120, Jan. 2019.

[12] J.-Y. Sung, C.-H. Yeh, C.-W. Chow, W.-F. Lin, and Y. Liu, "Orthogonal frequency-division multiplexing access (OFDMA) based wireless visible light communication (VLC) system," *Opt. Commun.*, vol. 355, pp. 261–268, Nov. 2015.

[13] M. Hammouda, A. M. Vegni, H. Haas, and J. Peissig, "Resource allocation and interference management in OFDMA-based VLC networks," *Phys. Commun.*, vol. 31, pp. 169–180, Dec. 2018.

[14] H. Marshoud, V. M. Kapinas, G. K. Karagiannidis, and S. Muhaidat, "Non-orthogonal multiple access for visible light communications," *IEEE Photon. Technol. Lett.*, vol. 28, no. 1, pp. 51–54, Jan. 1, 2016.

[15] L. Yin, W. O. Popoola, X. Wu, and H. Haas, "Performance evaluation of non-orthogonal multiple access in visible light communication," *IEEE Trans. Commun.*, vol. 64, no. 12, pp. 5162–5175, Dec. 2016.

[16] H. Marshoud, P. C. Sofotasios, S. Muhaidat, G. K. Karagiannidis, and B. S. Sharif, "On the performance of visible light communication systems with non-orthogonal multiple access," *IEEE Trans. Wireless Commun.*, vol. 16, no. 10, pp. 6350–6364, Oct. 2017.

[17] B. Lin, Z. Ghassemlooy, X. Tang, Y. Li, and M. Zhang, "Experimental demonstration of optical MIMO NOMA-VLC with single carrier transmission," *Opt. Commun.*, vol. 402, pp. 52–55, Nov. 2017.

[18] C. Chen, W.-D. Zhong, H. Yang, and P. Du, "On the performance of MIMO-NOMA-based visible light communication systems," *IEEE Photon. Technol. Lett.*, vol. 30, no. 4, pp. 307–310, Feb. 15, 2018.

[19] H. Ren *et al.*, "Performance improvement of NOMA visible light communication system by adjusting superposition constellation: A convex optimization approach," *Opt. Exp.*, vol. 26, no. 23, pp. 29796–29806, Nov. 2018.

[20] C. Chen, W.-D. Zhong, H. Yang, P. Du, and Y. Yang, "Flexible-rate SIC-free NOMA for downlink VLC based on constellation partitioning coding," *IEEE Wireless Commun. Lett.*, vol. 8, no. 2, pp. 568–571, Apr. 2019.

[21] Z. Ding, X. Lei, G. K. Karagiannidis, R. Schober, J. Yuan, and V. K. Bhargava, "A survey on non-orthogonal multiple access for 5G networks: Research challenges and future trends," *IEEE J. Sel. Areas Commun.*, vol. 35, no. 10, pp. 2181–2195, Oct. 2017.

[22] E. M. Almohimmah, M. T. Alresheedi, A. F. Abas, and J. Elmirghani, "A simple user grouping and pairing scheme for non-orthogonal multiple access in VLC system," in *Proc. 20th Int. Conf. Transparent Opt. Netw. (ICTON)*, Jul. 2018, pp. 1–4, Paper Tu.B2.3.

[23] M. B. Janjua, D. B. da Costa, and H. Arslan, "User pairing and power allocation strategies for 3D VLC-NOMA systems," *IEEE Wireless Commun. Lett.*, vol. 9, no. 6, pp. 866–870, Jun. 2020.

[24] S. R. Teli, S. Zvanovec, and Z. Ghassemlooy, "Optical Internet of Things within 5G: Applications and challenges," in *Proc. IEEE Int. Conf. Internet Things Intell. Syst. (IOTAIS)*, Nov. 2018, pp. 40–45.

[25] H.-S. Kim, D.-R. Kim, S.-H. Yang, Y.-H. Son, and S.-K. Han, "Mitigation of inter-cell interference utilizing carrier allocation in visible light communication system," *IEEE Commun. Lett.*, vol. 16, no. 4, pp. 526–529, Apr. 2012.

[26] S.-Y. Jung, D.-H. Kwon, S.-H. Yang, and S.-K. Han, "Inter-cell interference mitigation in multi-cellular visible light communications," *Opt. Exp.*, vol. 24, no. 8, p. 8512, Apr. 2016.

[27] H. Le Minh *et al.*, "100-Mb/s NRZ visible light communications using a postequalized white LED," *IEEE Photon. Technol. Lett.*, vol. 21, no. 15, pp. 1063–1065, Aug. 1, 2009.

[28] Y.-F. Liu, Y.-C. Chang, C.-W. Chow, and C.-H. Yeh, "Equalization and pre-distorted schemes for increasing data rate in in-door visible light communication system," in *Proc. Opt. Fiber Commun. Conf. (OFC)*, 2011, pp. 1–3, Paper JWA083.

[29] C. Chen, W.-D. Zhong, and D. Wu, "Indoor OFDM visible light communications employing adaptive digital pre-frequency domain equalization," in *Proc. Conf. Lasers Electro-Opt. (CLEO)*, Jun. 2016, pp. 1–2, Paper JTh2A.118.
[30] M. D. Soltani, X. Wu, M. Safari, and H. Haas, "Bidirectional user throughput maximization based on feedback reduction in LiFi networks," *IEEE Trans. Commun.*, vol. 66, no. 7, pp. 3172–3186, Jul. 2018.
[31] L. Zeng *et al.*, "High data rate multiple input multiple output (MIMO) optical wireless communications using white led lighting," *IEEE J. Sel. Areas Commun.*, vol. 27, no. 9, pp. 1654–1662, Dec. 2009.
[32] J. M. Kahn and J. R. Barry, "Wireless infrared communications," *Proc. IEEE*, vol. 85, no. 2, pp. 265–298, Feb. 1997.
[33] A. Mostafa and L. Lampe, "Physical-layer security for MISO visible light communication channels," *IEEE J. Sel. Areas Commun.*, vol. 33, no. 9, pp. 1806–1818, Sep. 2015.
[34] H. Tabassum and E. Hossain, "Coverage and rate analysis for co-existing RF/VLC downlink cellular networks," *IEEE Trans. Wireless Commun.*, vol. 17, no. 4, pp. 2588–2601, Apr. 2018.
[35] V. Papanikolaou, P. Diamantoulakis, Z. Ding, S. Muhaidat, and G. Karagiannidis, "Hybrid VLC/RF networks with non-orthogonal multiple access," in *Proc. IEEE Global Commun. Conf. (GLOBECOM)*, Dec. 2018, pp. 1–6.
[36] X. Wu, M. D. Soltani, L. Zhou, M. Safari, and H. Haas, "Hybrid LiFi and WiFi networks: A survey," 2020, *arXiv:2001.04840*. [Online]. Available: http://arxiv.org/abs/2001.04840
[37] H. Abuella *et al.*, "Hybrid RF/VLC systems: A comprehensive survey on network topologies, performance analyses, applications, and future directions," 2020, *arXiv:2007.02466*. [Online]. Available: http://arxiv.org/abs/2007.02466
[38] X. Zhang, Q. Gao, C. Gong, and Z. Xu, "User grouping and power allocation for NOMA visible light communication multi-cell networks," *IEEE Commun. Lett.*, vol. 21, no. 4, pp. 777–780, Apr. 2017.
[39] H. Tabassum, M. S. Ali, E. Hossain, M. J. Hossain, and D. I. Kim, "Uplink vs. downlink NOMA in cellular networks: Challenges and research directions," in *Proc. IEEE 85th Veh. Technol. Conf. (VTC Spring)*, Jun. 2017, pp. 1–7.
[40] L. Zhu, J. Zhang, Z. Xiao, X. Cao, and D. O. Wu, "Optimal user pairing for downlink non-orthogonal multiple access (NOMA)," *IEEE Wireless Commun. Lett.*, vol. 8, no. 2, pp. 328–331, Apr. 2019.
[41] V.-P. Bui, P. Nguyen, H. Nguyen, V.-D. Nguyen, and O.-S. Shin, "Optimal user pairing for achieving rate fairness in downlink NOMA networks," in *Proc. Int. Conf. Artif. Intell. Inf. Commun.*, Feb. 2019, pp. 575–578.

Chen Chen (Member, IEEE) received the B.S. and M.Eng. degrees from the University of Electronic Science and Technology of China, Chengdu, China, in 2010 and 2013, respectively, and the Ph.D. degree from Nanyang Technological University, Singapore, in 2017. He was a Post-Doctoral Researcher with the School of Electrical and Electronic Engineering, Nanyang Technological University, from 2017 to 2019. He is currently a Tenure-Track Assistant Professor with the School of Microelectronics and Communication Engineering, Chongqing University, Chongqing, China. His research interests include optical wireless communication, optical access networks, Internet of Things, and machine learning.

Shu Fu received the Ph.D. degree in communication and information system from the University of Electronic Science and Technology of China, Chengdu, China, in June 2016, with a focus on cooperative multi-point (CoMP) wireless network, QoS routing in wavelength division multiplexing (WDM) network, and cross-network energy efficiency. He is currently an Associate Professor with the School of Microelectronics and Communication Engineering, Chongqing University, Chongqing, China. His research interests include the next generation of wireless networks, integrated networks, and network virtualization.

Xin Jian received the B.Eng. and Ph.D. degrees from Chongqing University, Chongqing, China, in 2009 and 2014, respectively. He is currently an Associate Professor with the School of Microelectronics and Communication Engineering, Chongqing University. His research interests include the Internet of Things, next-generation mobile communication, and wireless ad hoc networks.

Min Liu received the B.Eng. and M.Eng. degrees from Chongqing University, Chongqing, China, in 1997 and 2000, respectively, and the Ph.D. degree from Nanyang Technological University, Singapore, in 2004. She is currently a Professor and the Vice Dean of the School of Microelectronics and Communication Engineering, Chongqing University. Her main research interests include optical fiber communication and photonic crystal fibers.

Xiong Deng (Member, IEEE) received the M.Eng. degree in communication and information engineering from the University of Electronic Science and Technology of China, in 2013, and the Ph.D. degree in optical wireless communications from the Eindhoven University of Technology, Eindhoven, The Netherlands, in 2018. In 2013, he was a Researcher with the Terahertz Science and Technology Research Center, China Academy of Engineering Physics, where he was involved in the integrated terahertz communication and imaging systems. He was a Guest Researcher with Signify (Philips Lighting) Research, where he was involved in light fidelity. He is currently a Post-Doctoral Researcher with the Eindhoven University of Technology. He serves as a Reviewer for multiple IEEE/OSA journals, including IEEE TRANSACTIONS ON INDUSTRIAL ELECTRONICS (TIE), IEEE JOURNAL OF EMERGING AND SELECTED TOPICS IN POWER ELECTRONICS (JESTPE), IEEE TRANSACTIONS ON COMPUTERS (TOC), IEEE TRANSACTIONS ON VEHICULAR TECHNOLOGY (TVT), IEEE JOURNAL OF LIGHTWAVE TECHNOLOGY (JLT), IEEE TRANSACTIONS ON COGNITIVE COMMUNICATIONS AND NETWORKING (TCCN), IEEE COMMUNICATIONS LETTERS (CL), and IEEE PHOTONICS JOURNAL (PJ). His research interests include the system modeling, digital signal processing, and circuits for intelligent lighting, millimeter wave, radio over fiber, and optical wireless communications.

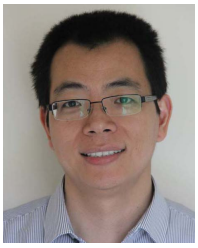

Zhiguo Ding (Fellow, IEEE) received the B.Eng. degree in electrical engineering from the Beijing University of Posts and Telecommunications, in 2000, and the Ph.D. degree in electrical engineering from Imperial College London, in 2005.

From July 2005 to April 2018, he was worked with Queen's University Belfast, Imperial College, Newcastle University, and Lancaster University. Since April 2018, he has been with The University of Manchester, as a Professor in communications. Since October 2012, he has also been an Academic Visitor with Princeton University. His research interests include B5G networks, machine learning, cooperative and energy harvesting networks, and statistical signal processing. He is serving as an Area Editor for IEEE Open Journal of the Communications Society, an Editor for IEEE TRANSACTIONS ON VEHICULAR TECHNOLOGY, and IEEE OPEN JOURNAL OF THE SIGNAL PROCESSING SOCIETY, and was an Editor for IEEE TRANSACTIONS ON COMMUNICATIONS, IEEE WIRELESS COMMUNICATION LETTERS, and IEEE COMMUNICATION LETTERS. He received the Best Paper Award in IET ICWMC-2009 and IEEE WCSP-2014, the EU Marie Curie Fellowship 2012–2014, the Top IEEE TVT Editor 2017, the IEEE Heinrich Hertz Award 2018, the IEEE Jack Neubauer Memorial Award 2018, the IEEE Best Signal Processing Letter Award 2018, and the Friedrich Wilhelm Bessel Research Award 2020. He is a Distinguished Lecturer of IEEE ComSoc, and a Web of Science Highly Cited Researcher in two categories 2020.